L ENGINEERING STUDIES
:tural Research Series No. 592

UILU-ENG-94-2011

ISSN: 0069-4274

AN OVERVIEW OF SELECTED SEISMIC HAZARD ANALYSIS METHODOLOGIES

By

Russell A. Green
and
William J. Hall

A Report on a Research Project
Sponsored by the
DEPARTMENT OF CIVIL ENGINEERING,
UNIVERSITY OF ILLINOIS AT URBANA-CHAMPAIGN

UNIVERSITY OF ILLINOIS AT URBANA-CHAMPAIGN
URBANA, ILLINOIS

August 1994

ABSTRACT

This report presents an overview of selected seismic hazard analysis (SHA) methodologies. First, background information about earthquakes is presented, followed by a more rigorous treatment of acceleration attenuation relationships. Commonly used expressions based on regression analysis and random vibration theory-band limited white noise (RVT-BLWN) are discussed.

Once the above preliminary information is given, the steps involved in determining site design PGAs are outlined for both deterministic and probabilistic seismic hazard analyses. Detailed examples of each approach are presented for the same fictitious site, allowing a comparison of the results to be made. Finally, a discussion on varying approaches for computing site design response spectra is presented. The examples for determining site PGAs are continued with site design spectra being computed using the reviewed methods.

ACKNOWLEDGEMENTS

This report is based on the dissertation of Russell A. Green submitted to the Graduate College, University of Illinois at Urbana-Champaign, for the degree of Master of Science in Civil Engineering. The thesis was completed under the supervision of Professor Emeritus William J. Hall.

The authors would like to express their sincere thanks to both the Civil Engineering Department, University of Illinois at Urbana-Champaign, for its support of this report, and the U.S. Defense Nuclear Facilities Safety Board (DNFSB) for its support of Russell Green.

The authors would also like to acknowledge the help and support of Professors Wilson Tang and Y.K. Wen, as well as, graduate students Kevin Collins and Ertugrul Taciroglu.

TABLE OF CONTENTS

LIST OF EXAMPLES

LIST OF TABLES

LIST OF FIGURES

CHAPTER 1
INTRODUCTION

1.1 Introduction and purpose of report

The occurrence of earthquakes poses a hazard to structures that can lead to disaster unless appropriate engineering countermeasures are employed. For special structures requiring more than the use of simplified seismic design procedures, such as those found in model building codes, a formal seismic hazard analysis (SHA) normally needs to be conducted on the prospective site before design begins. Inherent in a SHA are geologic and seismological investigations that provide site-specific information pertaining to the design ground motion. This information is required if a rigorous dynamic analysis of the proposed structure is to be performed as part of the design process.

This report provides an overview of steps involved in some of the current SHA methodologies. Although many papers have been written on this subject, the authors feel that this report is unique in its step-by-step detailed presentation of material not found in most articles published in technical journals. Furthermore, few courses, if any, are taught on SHA at universities, and therefore if the topic is included in a text it is generally only a cursory presentation.

The intended reader of this paper is the novice in SHA (e.g., a structural engineer who is familiar with structural dynamics and the use of design spectra, but knows little about seismology and the procedures used in determining design ground motion). Accordingly, background information about earthquakes, such as generating mechanisms and various earthquake measurement scales, is presented in Chapter 2. Also, tables are presented that allow the comparison of different magnitude scales for both plate boundary and interior plate earthquakes.

Discussions on geologic factors that influence seismic wave attenuation and the general approaches used in deriving

attenuation relationships are presented in Chapter 3. Furthermore, four expressions which are representative of most types of relationships currently used in practice also are presented. At the end of the chapter, plots are shown that compare the outputs of the four expressions for two different magnitudes; the significance of the two magnitudes used in these plots becomes apparent in Example 4.1.

The steps involved in both deterministic seismic hazard analysis (DSHA) and probabilistic seismic hazard analyses (PSHA) are outlined in Chapters 4 and 5, respectively. A detailed example is presented at the end of each chapter which illustrates the respective approaches; the same site is used in both examples to allow a comparison of the results. From these examples, the reader can gain insight into the effort required in performing a SHA.

In Chapter 6, descriptions of various types of design spectra and the theory behind each are presented. Also, the examples presented at the end of Chapters 4 and 5 are continued with the computation of the site's design spectra. Closing remarks are provided in Chapter 7.

As a final note, it is important to recognize that the field of ground motion specification is in the state of evolution. With the occurrence of new earthquakes and better instrumentation, the approaches and assumptions of SHA are continually being reanalyzed. As a result, many statements made in this report are prefaced with "generally," "usually," "typically," and other similar phrases; therefore what is presented should be looked upon only as a general overview and not as a definitive set of procedures to which all SHA strictly adhere.

CHAPTER 2
BACKGROUND INFORMATION ABOUT EARTHQUAKES

2.1 Plate tectonics

The basic premise of the theory of plate tectonics is that approximately 12 major slabs or plates make up the outer 70-150km of the earth (also known as the crust or lithosphere). Although it is known that these plates are slowly moving, the driving forces are not fully understood; it is hypothesized that the material directly below the crust, known as the asthenosphere, is churning as a result of temperature differentials throughout its depth [Gere, 1984; Hay, 1984; McKenzie, 1980].

The relative motion of the boundaries of adjacent plates causes rocks to strain. The strained rocks eventually rupture and rebound, thus creating an earthquake. Seismic events generated in this manner are referred to as tectonic earthquakes, and can occur either at the edges or interior of the plates. In the United States, edge-plate earthquakes result when plates either slide past each other or one underneath another. The motion along the San Andreas fault in California is an example of the situation where plates slide past each other. The focus, or location where fault rupture initiates, for earthquakes generated by this type of mechanism is usually less than 35 km deep; such earthquakes are referred to as shallow crustal earthquakes.

Earthquakes generated when one plate slides underneath another are referred to as subduction zone earthquakes. Focal depths for these earthquakes typically range from 25-700 km. An example of a subduction zone is the Aleutian island chain in Alaska. The distinction between these two types of earthquake mechanisms (i.e., shallow crustal and subduction zone) is made because the characteristic earthquake ground motion associated with each is different, with the latter usually producing larger shocks.

Although earthquakes occur most often on plate boundaries, a small percentage occur on plate interiors. It is believed that interior earthquakes are caused by a buildup of strain from pressures developed at the plate boundaries. Examples of large interior-plate earthquakes include the 1811-1812 New Madrid, Missouri, and the 1886 Charleston, South Carolina, earthquakes [Gere, 1984].

2.2 Measuring earthquake strength

There are two basic approaches to measuring the strength of an earthquake (i.e., magnitude and intensity). An earthquake's magnitude is a measure of the strain energy released during the event, and its determination is solely dependant on the analysis of seismograms/accelerograms. Intensity is a qualitative measure of earthquake induced effects at any geographic location. It should be emphasized that a point source earthquake has a fixed magnitude, but in general, its intensity decreases with distance from the epicenter. (The epicenter is the point on the earth's surface directly above the focus.)

Numerous scales are used to measure the magnitude of an earthquake. The first successfully applied scale was developed in 1935 by Professor Charles Richter, of the California Institute of Technology. The original Richter magnitude, M_L, (also known as Local magnitude) was defined as "...the logarithm to base ten of the maximum seismic-wave amplitude (in thousandths of a millimeter) recorded on a standard seismograph at a distance of 100 kilometers from the earthquake epicenter" [Bolt, 1988]. Figure 2.1 shows the steps involved in calculating the Richter magnitude (M_L) for a given earthquake.

Professor Beno Gutenburg, also of the California Institute of Technology, modified the approach in order to apply it to larger, more distant earthquakes; as a result, a new scale called Surface Wave magnitude (M_S) was created. It should be noted that both M_L and M_S scales are logarithmic; therefore, each increment in magnitude corresponds to a factor of 10 increase in

the amplitude of ground motion, all other factors being constant. Furthermore, for every increment in magnitude there is a factor of approximately 31.5 increase in released energy. The large increase in released energy relative to ground motion stems from the fact that only a portion of the energy released during a seismic event is in the form of seismic waves, the rest being in the form of heat [Gere, 1984; Hay, 1984]. Seismic body waves that radiate from the focus are either P waves (primary/compressional/dilatational) or S waves (secondary/ shear/distortional). The wave forms become more complex as they reflect, refract, combine, and take different travel paths.

Magnitude scales other than Local magnitude and Surface Wave magnitude include Body Wave magnitude (m_b and m_{blg}), and Moment magnitude (M_w). The Body Wave magnitude is measured as the common logarithm displacement amplitude in microns of the P-wave with period near one second. The value was developed to measure the magnitude of deep focus earthquakes which do not ordinarily set up detectable surface waves with long periods. Body wave magnitudes can be assigned from any suitable instrument whose constants are known. The body waves can be measured from either the first few cycles of compression waves (m_b) or the 1-second period shear waves (m_{blg}).

The Moment magnitude (M_w) is a function of Seismic moment (M_o). Seismic moment is an indirect measure of earthquake energy, and is considered to provide a more accurate measurement than other magnitude scales. For example, other magnitude scales saturate at given magnitude values (i.e., for further increases in the size of earthquakes, there is little or no increase in the magnitude values). Consequently, M_o (and its related magnitude) have become the preferred scale. The seismic moment is defined as:

$$M_o = G\ A\ D,$$

where G = rigidity modulus (resistance to shearing motion),
A = area of fault movement, and
D = average static displacement (slip).

The units typically associated with values of seismic moment are dyne-centimeters. One expression that relates seismic moment to moment magnitude is:

$$M_w = 2/3 \log M_o - 10.7$$

Tables 2.1 and 2.2 present comparisons among various scales for edge-plate earthquakes and interior plate earthquakes, respectively [Krinitzsky, 1993a].

Although there are many different intensity scales, the Modified Mercalli Intensity (MM or MMI) is the one most commonly used in the United States. As shown in Table 2.3, it consists of 12 different intensity levels that are derived from eyewitness accounts and damage assessments. Although pockets of abnormal effects can be formed, the intensity level of an earthquake generally decreases with distance from the epicenter. The rate at which the intensity levels decrease is a function of many parameters. A more detailed discussion of seismic wave attenuation is presented in Chapter 3.

2.3 Parameters of engineering interest

Around the world, an estimated 18,000-22,000 earthquakes of M_L greater than 2.5 occur each year. Fortunately, only a few of these are large enough to cause damage [Bolt, 1977]. Usually, only earthquakes of Richter magnitude (M_L) greater than 5.0 are of engineering concern.

Because earthquakes of the same magnitude can have different characteristics, peak ground acceleration, peak ground velocity, peak ground displacement, duration of strong ground motion, etc. are used to further describe an event. An attenuation expression is used to relate ground motion parameters to distance for a given magnitude event and geologic conditions. More details about these relationships are provided in Chapter 3.

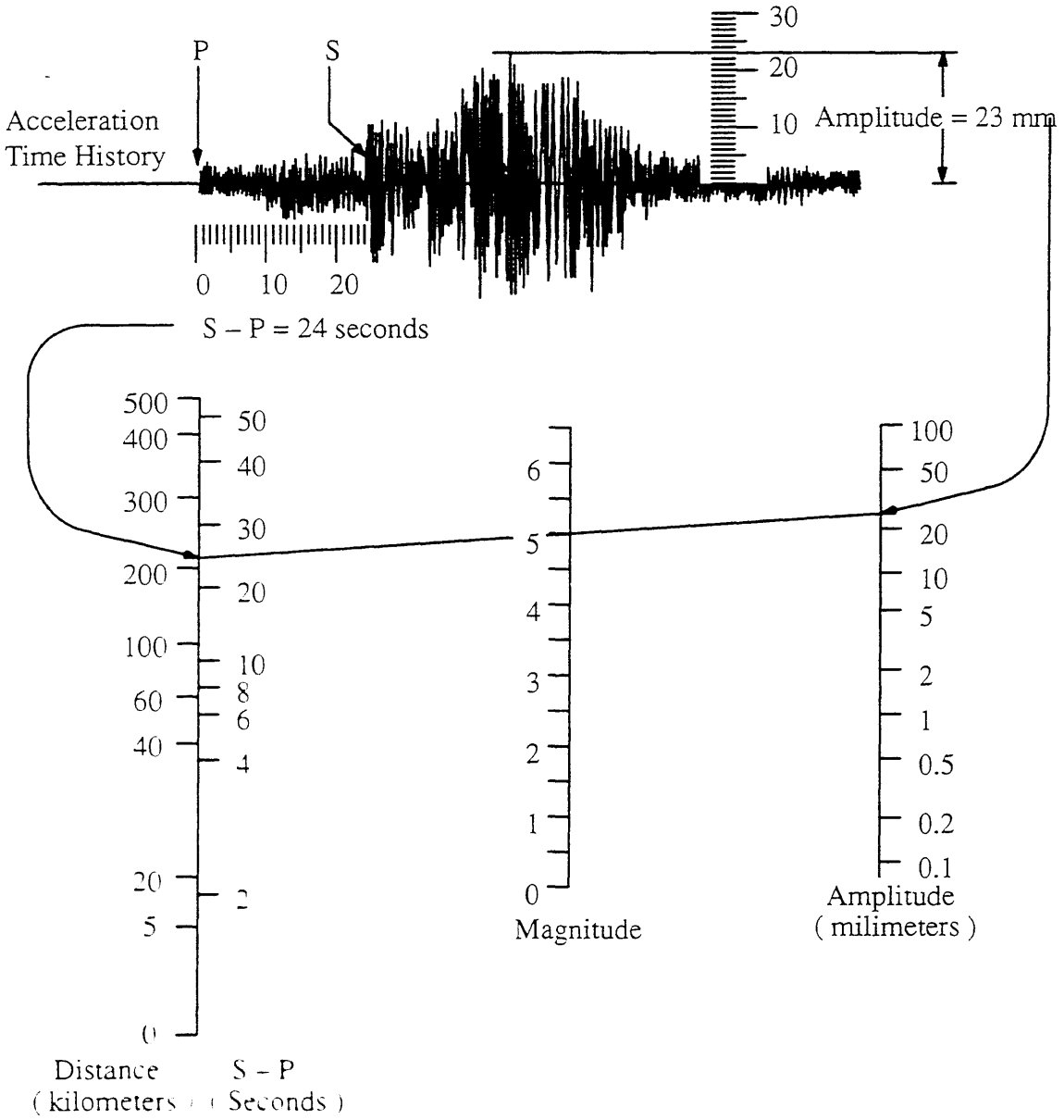

Procedure for calculating the local magnitude , M_L

1. Measure the distance to the focus using the interval time between the S and the P waves (S – P = 24 seconds)
2. Measure the height of the maximum wave motion on seismogram (23 milimeters)
3. Place a straight edge between appropriate points on the distance (left) and amplitude (right) scales to obtain magnitude M_L = 5.0.

Figure 2.1 Example of the calculation of the Richter magnitude (M_L) of a local earthquake (after Bolt,1988).

m_b	M_L	M_S	M_W	M_o (dyne-cm)	Epicentral Intensity I_o
4.0	4.3	3.0	4.1	10^{21}	IV
4.5	4.8	3.6	4.5	10^{22}	V
5.0	5.3	4.6	5.2	10^{23}	VI
5.5	5.8	5.6	5.8	10^{24}	VII
6.0	6.3	6.6	6.6	10^{25}	VIII
6.5	6.8	7.3	7.3	10^{26}	IX-X
7.0	7.3	8.2	8.2	10^{27}	XI-XII

Table 2.1 Equivalences between magnitude scales and intensity for *plate boundary* earthquakes [Krinitzsky, 1993a; Nuttli, 1987].

m_b	M_L*	M_S	M_W	M_o (dyne-cm)	Epicentral Intensity I_o
4.0	-	2.9	3.8	10^{21}	IV
4.5	-	3.4	4.1	10^{22}	V
5.0	-	4.4	4.8	10^{23}	VI
5.5	-	5.4	5.4	10^{24}	VII
6.0	-	6.4	6.1	10^{25}	VIII
6.5	-	7.4	6.8	10^{26}	IX-X
7.0	-	8.4	7.4	10^{27}	XI-XII

Table 2.2 Equivalences between magnitude scales and intensity for *interior plate* earthquakes [Krinitzsky, 1993a; Nuttli, 1987].

* M_L generally not used in plate interior.

I	Not felt except by a very few under especially favorable conditions.
II	Felt only by a few persons at rest, especially on upper floors of buildings. Delicately suspended objects may swing.
III	Felt quite noticeably indoors, especially on upper floors of buildings, but many people do not recognize it as an earthquake. Standing automobiles may rock slightly. Vibration like passing of truck. Duration can be estimated.
IV	During the day felt indoors by many, outdoors by few. At night some awakened. Dishes, windows, doors disturbed; walls make cracking sound. Sensation like heavy truck striking building. Standing automobiles rocked noticeably.
V	Felt by nearly everyone; many awakened. Some dishes, and other fragile items broken; a few instances of cracked plaster; unstable objects overturned. Disturbance of trees, poles and other tall objects sometimes noticed. Pendulum clocks may stop.
VI	Felt by all; many frightened and run outdoors. Some heavy furniture moved; a few instances of fallen plaster or damaged chimneys. Damage slight.
VII	Everybody runs outdoors. Damage negligible in buildings of good design and construction; slight to moderate in well-built ordinary structures; considerable in poorly built or badly designed structures. Some chimneys broken. Noticed by persons driving automobiles.
VIII	Damage slight in specially designed structures; considerable in ordinary substantial buildings with partial collapse. Great damage in poorly built structures. Panel walls thrown out of frame structures. Fall of chimneys, factory stacks, columns, monuments, walls. Heavy furniture overturned. Sand and mud ejected in small amounts. Changes in well water. Persons driving automobiles disturbed.

Table 2.3 Modified Mercalli Intensity (MMI) scale [Krinitzsky, 1993a].

IX	Damage considerable in specially designed structures; well designed frame structures thrown out-of-plumb; damage in substantial buildings, with partial collapse. Buildings shifted off foundations. Ground cracked conspicuously. Underground pipes broken.
X	Some well built wooden structures destroyed; most masonry and frame structures destroyed. Ground badly cracked. Railroad rails bent. Many landslides on river banks and steep slopes. Shifted sand and mud. Water splashed over banks of rivers and lakes.
XI	Few structures remain standing. Unreinforced masonry structures are nearly totally destroyed. Bridges destroyed. Broad fissures in ground. Underground pipe lines completely out of service. Earth slumps and land slips in soft ground. Railroad rails bent greatly.
XII	Damage total. Waves apparently seen on ground surfaces. Lines of sight appear visually destroyed. Objects thrown upward into the air.

Table 2.3 (continued) Modified Mercalli Intensity (MMI) scale [Krinitzsky, 1993a].

CHAPTER 3
ATTENUATION RELATIONSHIPS

3.1 Introduction

An attenuation expression provides a functional relationship between earthquake properties (e.g., peak ground acceleration) or response quantities (e.g., spectral response values) and various parameters such as magnitude, soil conditions, site-to-source distance, etc. Although many response quantities are useful, traditionally peak acceleration is most commonly used in engineering applications. After a description of the variables influencing attenuation and the varying forms of relationships, four typical expressions are examined.

3.2 Variables that affect attenuation

The attenuation of seismic waves is a function of a number of variables which generally can be categorized as: source mechanism, travel path, and local conditions. Each of these categories can be expanded further. For example, source mechanism encompasses factors such as stress and strain conditions, rupture dimensions, and source depth. Inclusive in travel path are such factors as geometric spreading, reflection, refraction, absorption, and geologic structure. Subsurface conditions, topographic variations, and soil-structure interaction all constitute local conditions. Although functional relationships that include all of the above factors are theoretically possible, the paucity of earthquake data precludes a true understanding of the exact influence of each factor [Idriss, 1978]. Two factors that often are represented in attenuation expressions are geometric spreading and absorption.

3.2.1 Geometric spreading and absorption

The inclusion of geometric spreading and absorption in many

relationships is possible because these phenomena are relatively well understood. The concept of geometric spreading can be easily illustrated when related to the conservation of energy. Spherical wave-fronts occupy more area as they progress from a seismic source. In keeping with the laws of conservation, the amplitude of the waves must decrease; hence, the mathematical expression that wave amplitudes decrease proportionally with $1/R^{\eta}$ is easily confirmed. In this mathematical expression, R is distance, and η is a constant dependent on travel path and geologic conditions [Reiter, 1990]. This expression is a generalization, and consideration needs to be given to influences from factors such as unusual geologic conditions. The effect which unusual geologic features can have is illustrated in the following analogy. Sunlight intensity decreases with distance from the sun, but can be locally focused if rays pass through a magnifying glass; the magnifying glass is analogous to unique geologic features [Lindeburg, 1990].

Absorption is more complex than geometric spreading. In general, absorption results from friction in the medium and scattering of the waves which can cause destructive interference. An often used expression that relates absorption to frequency and rock properties is $Q = Q_o f^n$, where Q is called the quality factor, f is frequency, and Q_o and n are constants dependent on rock properties. Large values of Q correspond to low absorption (and attenuation), and vice-versa. Observations have shown that seismic waves are attenuated less in the overlying mantle in the eastern United States (US) as opposed to the folded and fractured mountainous topography of the western US [Reiter, 1990]. In extending the above sunlight analogy, the earth is spared from many harmful cosmic rays that are absorbed in its atmosphere.

3.3 Types of attenuation relationships

The actual functional form of an attenuation expression depends on the approach used to derive it or the theory on which

it is based. In general, most expressions are variations of two types. While many names have been used to title these two categories, in this paper they are referred to as empirical and theoretical. As will be seen subsequently, these titles are somewhat ambiguous because many empirical type expressions contain theoretically based terms, and many theoretical type relationships incorporate empirically derived constants.

The distinction between empirical and theoretical expressions is as follows. Empirical type relationships are typically derived by applying regression analysis methods to observed and recorded earthquake data. On the other hand, theoretical expressions attempt to model directly the physics of earthquakes and related mechanisms, with constants being determined empirically. In some cases, the distinction as to whether an expression is empirical or theoretical is difficult to discern.

3.3.1 Empirical attenuation relationships

The following discussion on empirical type attenuation expressions is limited to those derived through regression analysis; most have the basic functional form:

$$Y = b_1 f_1(M) f_2(R) f_3(M,R) f_4(P_i) \epsilon,$$

where Y = strong motion parameter, (e.g. peak acceleration),

b_1 = constant scaling factor,

$f_1(M)$ = a function of the independent variable M, (magnitude or earthquake source size),

$f_2(R)$ = a function of the independent variable R, (site-to-source distance),

$f_3(M,R)$ = a joint function of the variables M and R,

$f_4(P_i)$ = function(s) representing possible source, site, and building effects, and

ϵ = an error term representing uncertainty in Y.

Based on observational evidence, Y is usually assumed to be log-normally distributed. This allows the above expression to be presented in the more useful additive form:

$$\ln Y = \ln b_1 + \ln f_1(M) + \ln f_2(R) + \ln f_3(M,R) + \ln f_4(P_i) + \ln \epsilon \ .$$

Attention needs to be directed as to which magnitude scale is used and how the site-to-source distance is defined (e.g., epicentral, hypocentral, etc.). Figure 3.1 illustrates the different site-to-source distances commonly used in attenuation relationships; the reader may refer back to Section 2.2 for a discussion on different magnitude scales.

Because many empirical type expressions employ regression techniques to existing data to determine constants and functions, the results are subject to the limitations of the specific records included in the analysis and the regression technique used. It should be noted that the same seismic event can be recorded at more than one recording site (i.e., one earthquake event can lead to many recorded accelerograms). Hence, even though the earthquake database may be composed of a relatively large number of records, its representation of different types of source mechanisms and geologic conditions is limited. The use of a disproportionate number of time histories from only one or two earthquakes can have unwarranted influence on the obtained relationships. Also, most recording stations provide two horizontal time histories for perpendicularly oriented directions. The method used in the treatment of these two related records in the analysis can significantly affect the results (e.g., the results can differ depending on whether or not the larger of the two horizontal components is used or if an averaging technique is employed, etc.).

Three empirical type attenuation expressions are described below, beginning with one of the earlier recognized relationships followed by two more modern ones. The first

expression to be examined was developed by Donovan and Bornstein (1978) for shallow crustal western earthquakes. Next, a relationship proposed by Crouse (1991) for northwestern subduction zone events is characterized. Lastly, Boore, Joyner, and Fumal's (1993) attenuation expression for shallow crustal western earthquakes is discussed.

3.3.1.1 Donovan and Bornstein (1978)

Although possibly outdated due to the increase in the seismic database since its development, Donovan and Bornstein's (1978) relationship is representative of earlier attenuation relationships. They proposed the following expression to estimate peak horizontal ground acceleration for rock and firm soil sites resulting from western shallow crustal earthquakes:

$$a = 2{,}154{,}000\, R^{-2.1}\, e^{(0.046 + 0.445 \log R)M}\, (R + 25)^{-(2.515 - 0.486 \log R)},$$

for $M \leq 8$; $R \geq 5$ km,

where a = median peak horizontal peak ground acceleration in gals (or cm/sec^2).

R = distance from the site to the center of energy on the causative fault in kilometers (km), and

M = magnitude.

The standard error of ln(a) ($\sigma_{\ln(a)}$) and the coefficient of variation of PGA (COV_{PGA}) of the above expression vary as function of acceleration:

Peak Horizontal Acceleration	$\sigma_{\ln(a)}$	COV_{PGA}
0.05g	0.48	0.51
0.10	0.46	0.49
0.15	0.41	0.43
≥ 0.30	0.30	0.31

The coefficient of variation (COV) often is employed because it

expresses the amount of dispersion in the data as a functional relationship between $\sigma_{meanPGA}$ and the mean value of the PGA (μ_{PGA}):

$$COV_{PGA} = \frac{\sigma_{meanPGA}}{\mu_{PGA}} , \quad COV_{PGA} = \sqrt{\exp(\sigma^2_{\ln(PGA)}) - 1} ,$$

where COV_{PGA} is the coefficient of variation of the PGA, $\sigma_{meanPGA}$ is the standard error of the mean PGA, $\sigma_{\ln(PGA)}$ is the standard error of ln(PGA) (or ln(Y)), and μ_{PGA} is the mean PGA. Assuming that the scatter of the data is log-normally distributed, median and mean values of PGA are related by the following expression:

$$\mu_{PGA} = PGA_{median} \times \sqrt{1 + COV^2_{PGA}} .$$

The COV is directly proportional the dispersion (or scatter) in the data used in the analysis.

No specific magnitude scale is stated for use, but based on a previous relationship presented by Donovan, the Richter magnitude (M_L) scale is assumed [Idriss, 1978]. (Note: Tables 2.1 and 2.2 provide a relative comparison of the different magnitude scales.) Also, note that the site-to-source distance defined for use with this expression is the distance from the site to the energy center on the causative fault (i.e., in Figure 3.1 this distance is labeled R_s). The center of energy is defined as the centroid of a high localized stress drop zone on the fault rupture plane.

The exact details as to which records were used and the regression technique employed in the derivation of this expression is beyond the scope of this report; such information is provided in the referenced reports [Donovan, 1978; Idriss, 1978].

3.3.1.2 Crouse (1991)

Crouse proposed the following expression to estimate

horizontal ground motion for the Cascadia subduction zone for shallow firm sites in the Pacific Northwest:

$$\ln(Y) = b_1 + b_2M + b_3M^2 + b_4 \ln\{R + b_5\exp(b_6M)\} + b_7h + \sigma,$$

where
- Y = median peak ground acceleration (gals),
- M = Moment magnitude,
- R = site to center of energy release distance (km),
- h = focal depth (km),
- b_1-b_7 = constants, and
- σ = standard error of ln(Y).

No distance limitations are given, but the site-to-source distance used in this equation is the distance from the site to center of energy release (i.e., R_5 in Figure 3.1). In the analysis of the earthquake records of $M \leq 7.5$, Crouse assumed the site to center of energy release distance to be approximately equal to the hypocentral distance, and for larger earthquakes this distance was assumed to be the site to centroid-of-fault-plane distance. With the appropriate values of b_{1-7} applied [Crouse, 1991], the above expression reduces to:

$$\ln Y = 6.36 + 1.76M - 2.73 \ln(R + 1.58e^{0.608M}) + 0.00916h + \sigma,$$
$$\sigma_{\ln(Y)} = 0.773, \text{ (i.e., } COV_{PGA} = 0.90) .$$

Note that as with the standard error for the Donovan and Bornstein (1978) relationship, the standard error for the above expression is for ln(Y) and not for Y; however, the value of COV_{PGA} is constant for this expression.

The details as to which records were used in the analysis and the method of regression employed in the derivation of this expression, can be found in the referenced report [Crouse, 1991].

3.3.1.3 Boore, Joyner, and Fumal (1993)

Boore, Joyner and Fumal have recently proposed the following relationship to estimate horizontal ground motion for shallow earthquakes in western North America:

$$\log_{10}(Y) = b_1 + b_2(M-6) + b_3(M-6)^2 + b_4 r + b_5 \log_{10}(r) + b_6 G_B + b_7 G_C + \sigma_{\log(Y)},$$

for $5.0 \leq M \leq 7.7$; $d \leq 100$ km,

where

$r = (R^2 + h^2)^{1/2}$,

Y = ground-motion quantity to be estimated (in cm/s for response spectra and g for peak acceleration.),

M = Moment magnitude of the earthquake,

R = the shortest distance (km) from the site of interest to the point on the earth's surface directly over the fault rupture, (note: if the site lies directly above a portion of the fault rupture, i.e., Figure 3.1, then R=0),

$G_{B\ \&\ C}$ = site classification coefficients,

$\sigma_{\log(Y)}$ = combined standard error of Y for each record and earthquake, and

b_{1-7} & h = constants.

In the use of this expression, a site is classified into one of four categories (A, B, C, and D) depending on the average shear-wave velocities of the upper 30m of geologic material. Classes A, B, C, and D include sites where the average shear-wave velocity are: greater than 750 m/s; between 360 m/s and 750 m/s; between 180 m/s and 360 m/s; and less than 180 m/s, respectively. As a result of lack of data presently available for site class D, Boore, Joyner, and Fumal excluded it from their analysis.

When the constants derived for estimating the peak acceleration for the larger of two horizontal components are substituted, the above equation reduces to:

$$\log_{10}(Y) = -0.038 + 0.216(M - 6) - 0.777 \log_{10}(R^2 + 30.03)^{1/2} + 0.158G_B + 0.254G_C$$

where $\sigma_{\log(Y)} = 0.205$ (i.e., $COV_{PGA} = 0.78$; the method outline in Section 3.3.1.1 above was used to compute the COV_{PGA} value for this expression, but the first $\sigma_{\log(Y)}$ was converted to $\sigma_{\ln(Y)}$ by using the following relationship: $\sigma_{\ln(Y)} = 2.303 \cdot \sigma_{\log(Y)}$). The site coefficient G_B equals one for site class B and zero otherwise. The same is true for G_C, with respect to site class C.

Again, the exact details of the derivation of this expression can be found in the referenced report [Boore, 1993].

3.3.2 Theoretical attenuation relationships

In contrast to empirical relationships that are typically derived by regression analysis of existing data, theoretical type expressions attempt to model physical properties directly. Even though these expressions are referred to as theoretical, empirically determined parameters are often required in order for many of these relationships to be employed. Because theoretical type expressions are less dependant on recorded data than empirical expressions, they often have been used in the eastern United States where records of large events are scarce.

The remaining discussion on theoretical attenuation relationships is limited to expressions based on Random Vibration Theory-Band Limited White Noise (RVT-BLWN). (Other theoretical type expressions such as those based on Green's function are not discussed in this report.) The use of RVT-BLWN came from the observation that acceleration time histories are, to a very good approximation, band-limited white Gaussian noise within the S-wave arrival window. The upper and lower band limitations are the spectral corner frequency (f_o) and the highest frequency passed by the earth or accelerograph (f_{max}). The parameter f_o is a function of the shear wave velocity near the source, and f_{max} is believed by seismologists to be either a

function of source properties or local site conditions [Reiter, 1990]. The theoretical type attenuation equation that will be examined in this paper was developed by Hanks and McGuire (1981).

3.3.2.1 Hanks and McGuire model (1981)

Hanks and McGuire proposed the following RVT-BLWN based theoretical model to estimate peak horizontal ground acceleration:

$$a_{max} = 10\left[0.85\frac{(2\pi)^2}{106}\frac{\Delta\sigma}{\rho R}\sqrt{\frac{f_{max}}{f_o}}\right]\sqrt{2\ln\left(\frac{2f_{max}}{f_o}\right)},$$

$$f_{max} = \frac{Q\beta}{\pi R};\quad f_o = 10^7\beta\sqrt[3]{\frac{\Delta\sigma}{8.5\times10^{(1.5M+16.0)}}},$$

where

a_{max}	=	peak ground acceleration (gals),
Q	=	quality factor,
ß	=	shear wave velocity (km/sec),
f_o	=	corner frequency (Hz),
f_{max}	=	maximum frequency passed by the earth or accelerograph (Hz),
ρ	=	density (gm/cm^3),
Δσ	=	earthquake stress drop or stress parameter (bars),
M_o	=	Seismic moment (dyne-cm),
M	=	Moment magnitude, and
R	=	hypocentral distance (km), (i.e., R_4 in Figure 3.1).

Both Δσ and f_o are parameters of the causative earthquake, while ρ, ß, and Q are parameters of the medium. The magnitude and distance ranges used in the referenced report are $4.0 \le M \le 6.5$, and $R \ge 10$ km, respectively. In the analysis of

California earthquakes records, Hanks and McGuire assumed the following values: ρ = 2.7 gm/cm^3, β = 3.2 km/sec, Q = 300, $\Delta\sigma$ = 100 bars. If one assumes these same values the above expression reduces to:

$$a_{max} = \frac{759.74 \times 10^{\left(\frac{M}{4} - \frac{5}{6}\right)}}{R^{3/2}} \sqrt{8.861 - 2 \ln[R \times 10^{\left(-\frac{M}{2} + \frac{5}{3}\right)}]} \ .$$

The assumptions used and the theory behind this relationship can be found in the referenced reports [Hanks, 1981; Reiter, 1990].

3.4 Closing remarks

Numerous other attenuation equations exist, many of which cannot be clearly labeled as either empirical or theoretical, but rather hybrids of the two. Many attenuation expressions use epicentral intensity to describe the size of the earthquake, as opposed to magnitude. Also, studies conducted by Professor Donald V. Helmberger, of the California Institute of Technology, currently are ongoing in the derivation of time-domain based attenuation relationships (as opposed to the frequency-domain based expressions, e.g., Hanks and McGuire, 1981). The four expressions presented above were selected only to show typical forms of acceleration attenuation relationships. Figure 3.2 shows plots of peak ground acceleration verses distance for Moment magnitudes 6.5 and 7.5 using each of the four relationships. The significance of these two magnitudes will become apparent after reviewing Example 4.1. When comparing the plots of the different expressions, it must be kept in mind the different magnitude scales, type of earthquake mechanism, distance relationships, and site conditions that is associated with each.

Examples 4.1 and 5.1 illustrate how attenuation relationships are used in a seismic hazard analysis. Also, a discussion on how some attenuation relationships can be employed

to directly calculate response spectra is presented in Chapter 6.

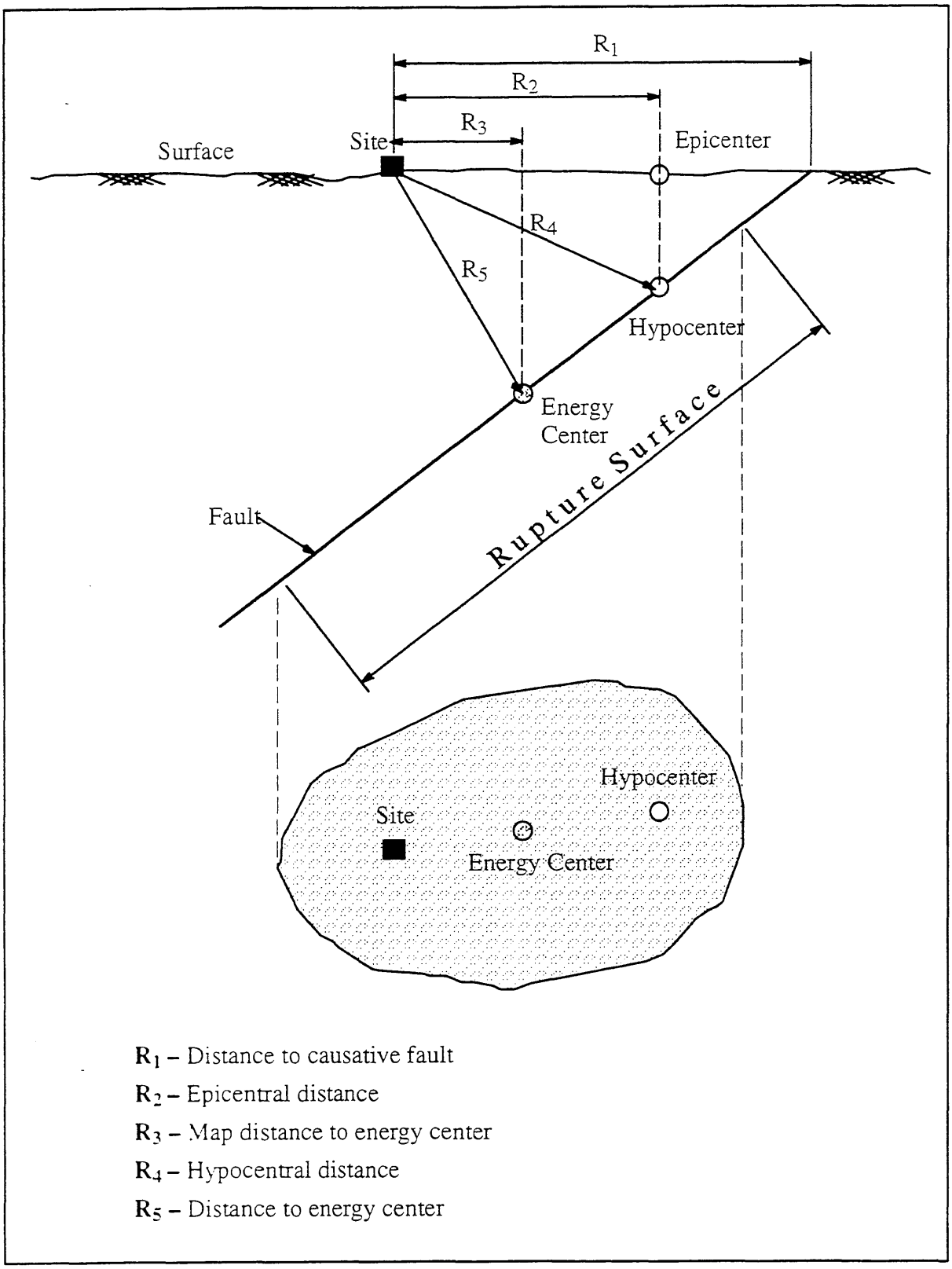

R_1 – Distance to causative fault

R_2 – Epicentral distance

R_3 – Map distance to energy center

R_4 – Hypocentral distance

R_5 – Distance to energy center

Figure 3.1 Site-to-source definitions (after Tri-Service manual, 1986).

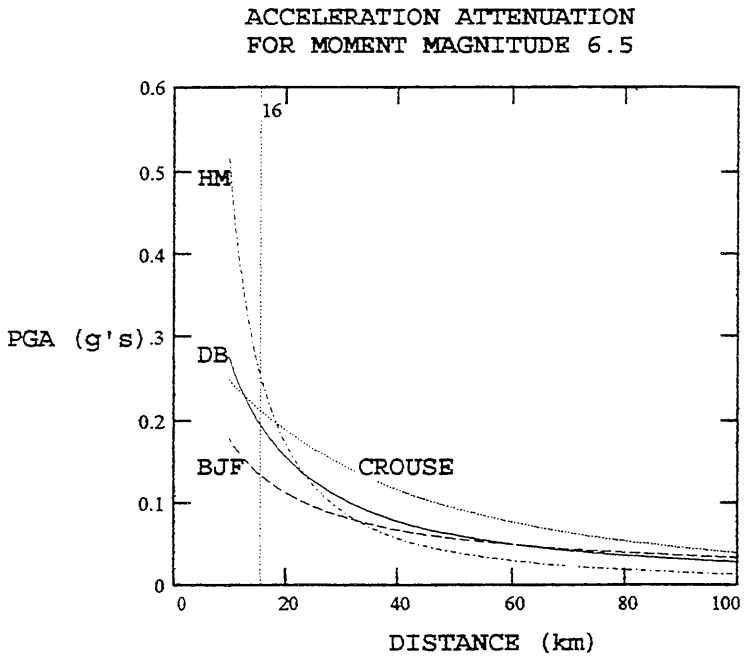

DB = Donovan and Bornstein (1978)
Crouse = Crouse (1991)
BJF = Boore, Joyner and Fumal (1993)
HM = Hanks and McGuire (1981)

NOTE: For Donovan and Bornstein a Richter magnitude of 6.24 is used, which is approximately equal to a moment magnitude of 6.5 (see Table 2.1). Also, Crouse (1991) is for a subduction zone earthquake with a focal depth of h=5 km.

Figure 3.2 PGA vs. distance for various attenuation expressions.

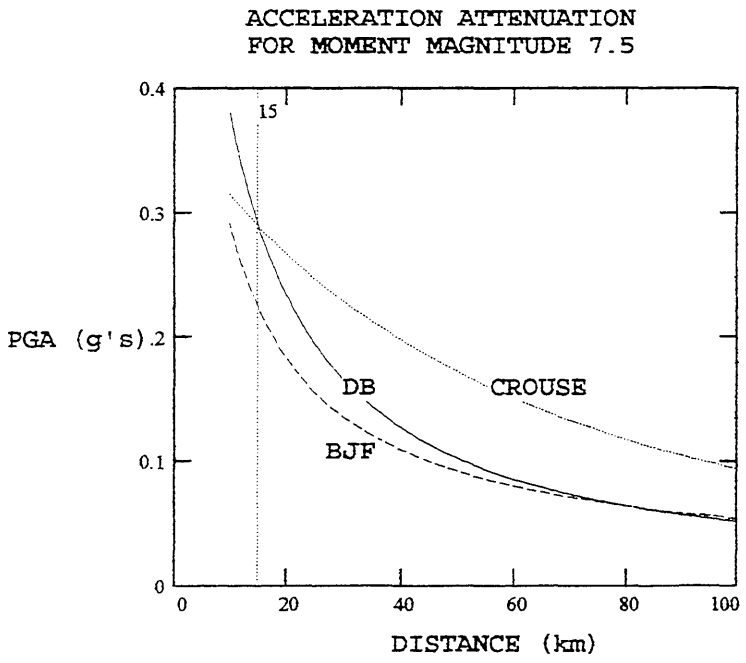

DB = Donovan and Bornstein (1978)
Crouse = Crouse (1991)
BJF = Boore, Joyner, and Fumal (1993)

NOTE: For Donovan and Bornstein a Richter magnitude of 6.9 is used, which is approximately equal to a moment magnitude of 7.5 (see Table 2.1). Hanks & McGuire is not shown because it has an upper magnitude limit of Mw = 6.5. Also, Crouse (1991) is for subduction zone earthquakes with a focal depth of h=5 km.

Figure 3.2 (continued).

CHAPTER 4
DETERMINISTIC SEISMIC HAZARD ANALYSIS

4.1 Introduction

The design ground motion at a site is determined by conducting a seismic hazard analysis (SHA). In general, a SHA can be classified as either deterministic or probabilistic depending on the approach taken. Outlined below are the steps involved in deterministic seismic hazard analyses (DSHA); one of which entails the use of the acceleration attenuation relationships discussed in Chapter 3. Example 4.1 is presented to help illustrate these steps. Probabilistic seismic hazard analysis (PSHA) is the topic of Chapter 5.

4.2 Steps involved in DSHA

In general, DSHA involves 4 basic steps: identification of sources; determination of the controlling earthquake for each source; selection of a ground motion relationship; and the computation of the design ground motion parameter(s). Figure 4.1 depicts these steps; each is discussed in sequential order below.

4.2.1 Step 1: Identification of sources

When a prospective site for a facility is being reviewed, all seismic sources that could produce damaging ground motion at the site need to be defined. Although a description of the exact procedures used in defining seismic sources is beyond the scope of this report, the identification process is based upon the interpretation of geological, geophysical, and seismological data. Sources can be represented by points, lines, and areas. However, most are defined as areas (or zones) because the preciseness of a point or line may not properly depict the knowledge (or lack of knowledge) of the earthquake mechanisms.

4.2.2 Step 2: Selection of the controlling earthquakes

Once all the sources are identified, the controlling earthquakes for each need to be determined. The definition of "controlling earthquake" is somewhat subjective and varies depending on the resulting hazard created if the prospective facility were to fail. For a facility whose failure only presents a relatively low hazard, the controlling earthquake might be defined as one that would be reasonably expected to occur during the operating life of the facility. Most national building codes in use today specify the design event as being one that has an expected return period of 475 years. For critical facilities -- facilities whose failures present high hazards (e.g., nuclear power plants, chemical plants, etc.) -- the controlling earthquake is usually defined as the maximum magnitude earthquake, m_{max}, that a given source is believed to be capable of generating.

Because the earthquake database in the United States only extends back several hundred years at best, the maximum historic earthquake for a region or source is usually used as a minimum value for m_{max}. Geologic investigations also are used to determine m_{max}. For example, correlations exist between surface fault length and maximum possible earthquakes. Furthermore, trenching a fault may determine the amount of slip and provide a clue as to the associated size of past events [Wells, 1994].

Each of the controlling earthquakes need to be paired with a site-to-source distance. As with the definition of "controlling earthquake," the definition of site-to-source distance is somewhat subjective. For example, if a fault that is identified as a potential seismic source has a portion that is considerably more active than the rest, one plausible measure of the site-to-source distance could be the distance from the site to the more active region on the fault. However, another plausible definition is the shortest distance from the site to *any* portion of the fault. For critical facilities the latter definition is usually employed. It should be noted that if the

site/source orientation is viewed in plan, the present discussion only pertains to the *angle* that a line which extends from the site to the source forms with a given direction in the same plane, and does not necessarily pertain to the *absolute* length of the line. The absolute length of the line is a function of both the angle described in the plan view and the point on the source where the line terminates (e.g., epicenter, hypocenter, etc.), which is particular to the attenuation relationship selected.

4.2.3 Step 3: Selection of a ground motion relationship

Peak ground acceleration (PGA) is the most common parameter used to describe ground motion. As discussed in Chapter 3, acceleration attenuation relationships relate magnitude and distance of a given event to the resulting PGA. An attenuation expression needs to be selected appropriately based on the type of source mechanism (e.g., shallow crustal, subduction, etc.).

As described in Chapter 3, and later herein, recent statistical studies of shallow crustal western earthquakes, e.g., [Boore, 1993], provide estimates of PGA as well as pseudo spectral relative velocity (S_{pv}).

4.2.4 Step 4: Computation of design ground motion parameters

The site design ground motion is determined by using the attenuation expression selected in Step 3 to compute the PGAs (assuming PGA is the parameter used to describe the site ground motion) corresponding to the controlling earthquakes (Step 2) associated with each source identified in Step 1. The earthquake associated with the largest of these site PGAs is typically used to define the site's design ground motion. As is discussed in Chapter 6, the design PGA can be used to scale a fixed-shape spectra, or its associated magnitude-distance pair can be used in conjunction with a spectral attenuation relationship to directly compute the site's design spectra [Clough, 1993; Krinitzsky, 1993b].

4.3 Description of Example 4.1

Figure 4.2 shows the orientation of a fictitious site with two identified sources (i.e., line and area) and their associated m_{max}. Example 4.1 uses this site to help illustrate the steps involved in a DSHA, which were outlined above. It should be noted that the site-to-source distances shown in Figure 4.2 are not necessarily the appropriate measurements defined for use with the Boore, Joyner, and Fumal (1993) attenuation expression which is used in this example, but they are used for pedagogical purposes.

> Note: the site-to-source distance defined for use with the Boore, Joyner, and Fumal (1993) attenuation expression is the shortest distance from the site of interest to the point on the earth's surface directly over the fault rupture. Hence, the below grade orientations of the sources are required in order for the appropriate site-to-source distances to be determined. In cases where an area source model is used because a fault trace can not be identified, often the source is assumed to have a vertical below grade orientation.

The problem definition of this example was taken from the Tri-Service manual, TM 5-809-10-1/NAVFAC P-355.1/AFM 88-3, **Seismic Design Guidelines For Essential Buildings, Change 1**, 1986, but the approaches used in determining the site hazard and the corresponding computations associated with both this example and Example 5.1, differ from those presented in the Tri-Service manual.

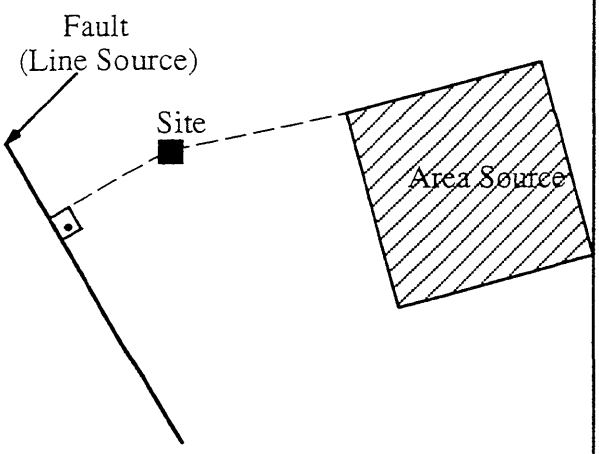

Step 1
IDENTIFICATION
OF SOURCES

FIXED DISTANCE **R**

FIXED MAGNITUDE **M**

FOR EACH SOURCE

Step 2
DETERMINE
CONTROLLING EARTHQUAKE
OF EACH SOURCE

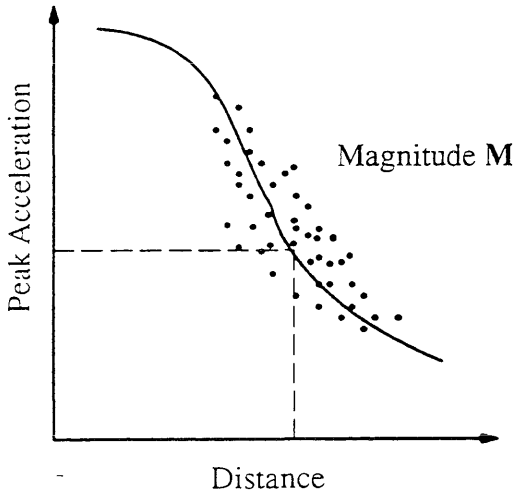

Step 3
SELECTION OF
GROUND MOTION
RELATIONSHIP

FIXED
PEAK
ACCELERATION
OR
OTHER GROUND
MOTION MEASURES

Step 4
COMPUTATION OF DESIGN
GROUND MOTION

Figure 4.1 Basic steps of deterministic seismic hazard analysis (after Reiter, 1990).

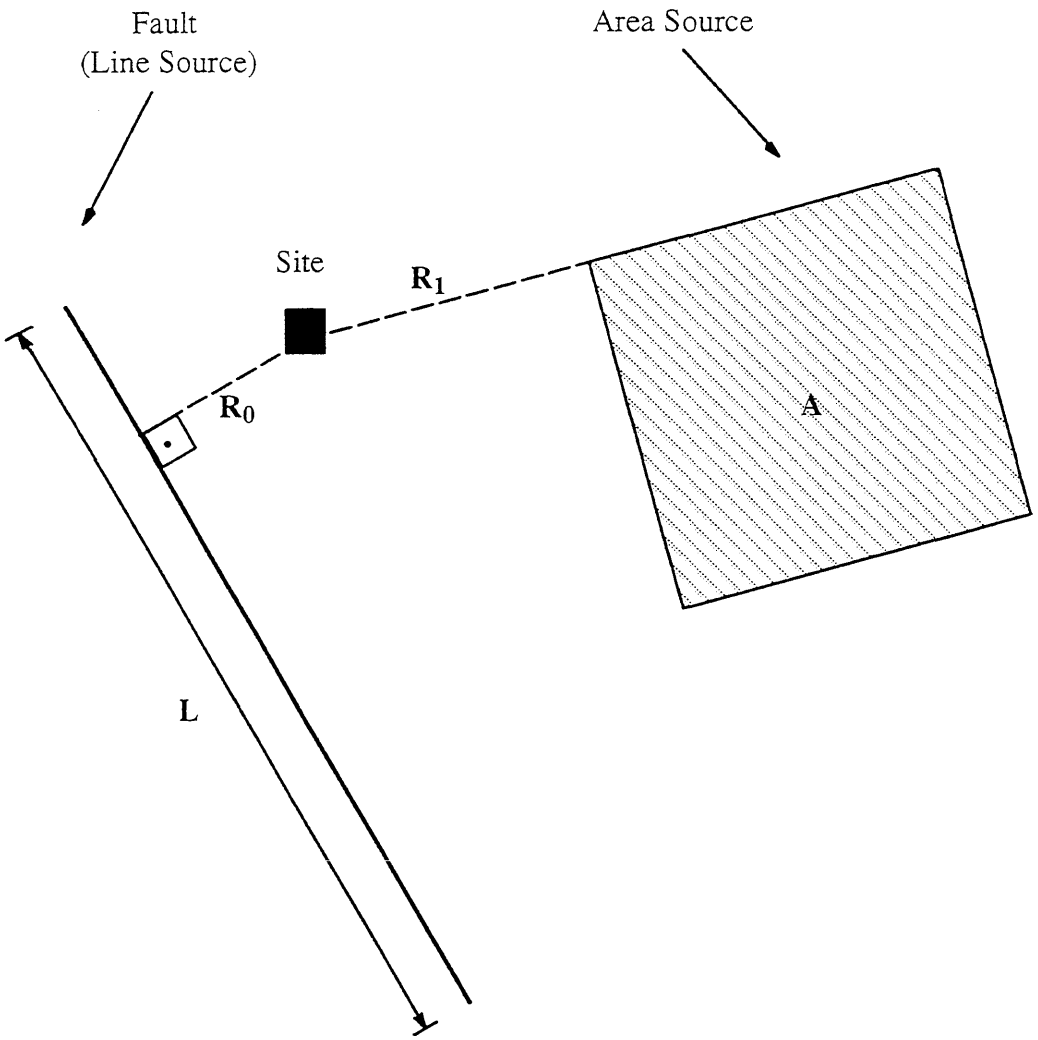

LINE SOURCE 1.

L = 30 km

R_0 = 15 km

m_{max} = 7.5

AREA SOURCE 2.

A = 400 km^2

R_1 = 16 km

m_{max} = 6.5

Figure 4.2 DSHA example (after Tri-Service manual,1986).

STEP 1: Indentification of sources: Two sources are indentified in this example, a line source and an area source (see Figure 4.2).

STEP 2: Selection of the controlling earthquakes for each source: In this example the controlling earthquake is defined as the maximum magnitude earthquake that a given source is capable of generating. The controlling earthquakes are Moment magnitudes 7.5 and 6.5 for the line source and area source, respectively. The controlling earthquakes are paired with the respective shortest site-to-source distances. For the line source the distance of 15 km is paired with the M = 7.5 event, and for the area source 16 km is paired with the M = 6.5 event.

STEP 3: Selection of the ground motion relationship: In this example the site PGA is used to describe the ground motion. The Boore, Joyner, and Fumal (1993) acceleration attenuation expression is used to determine the resulting site PGA from each source's controlling earthquake [Boore, 1993].

$$\log PGA = b_1 + b_2 \cdot (M - 6) + b_3 \cdot (M - 6)^2 + b_4 \cdot \sqrt{(R)^2 + h^2}$$
$$+ b_5 \cdot \log\left(\sqrt{R^2 + h^2}\right) + b_6 \cdot G_B + b_7 \cdot G_C$$

STEP 4: Computation of design ground motion parameter: The controlling earthquakes and associated site-to-source distances determined in Step 2 are plugged into the ground motion expression selected in Step 3 to compute the resulting site PGA's for each source. In this example the magnitude distance pair that results in the largest site PGA is used for the design parameter.

Example 4.1 Deterministic seismic hazard analysis (DSHA).

LINE SOURCE:

$b_1 := -0.038$ $b_2 := 0.216$ $b_3 := 0.0$ $b_4 := 0.0$ $b_5 := -0.777$ $b_6 := 0.158$

$b_7 := 0.254$ $h := 5.48$ $G_B := 0.0$ $G_C := 0.0$ $M_1 := 7.5$ $R_1 := 15$

$$\log PGA_1 := -0.038 + 0.216 \cdot (7.5 - 6) - 0.777 \cdot \log\left(\sqrt{15^2 + 5.48^2}\right)$$

$$\log PGA_1 = -0.649$$

$$PGA_1 := 10^{\log PGA_1}$$

$$PGA_1 = 0.22 \quad g$$

AREA SOURCE:

$b_1 := -0.038$ $b_2 := 0.216$ $b_3 := 0.0$ $b_4 := 0.0$ $b_5 := -0.777$ $b_6 := 0.158$

$b_7 := 0.254$ $h := 5.48$ $G_B := 0.0$ $G_C := 0.0$ $M_2 := 6.5$ $R_2 := 16$

$$\log PGA_2 := -0.038 + 0.216 \cdot (6.5 - 6) - 0.777 \cdot \log\left(\sqrt{15^2 + 5.48^2}\right)$$

$$\log PGA_2 = -0.884$$

$$PGA_2 := 10^{\log PGA_2}$$

$$PGA_2 = 0.13 \quad g$$

The larger of the resulting PGAs is from the line source's controlling earthquake (e.i., M = 7.5, R = 15 km); therefore the design ground motion parameter is PGA = 0.22g. (Note: the above PGAs are median values; other specified values also may be used.)

Example 4.1 (continued).

CHAPTER 5
PROBABILISTIC SEISMIC HAZARD ANALYSIS

5.1 Introduction

As described in Chapter 4, the design ground motion in a deterministic seismic hazard analysis (DSHA) results from only a single magnitude earthquake, on a single source, at a single distance from the site, without regard to the likelihood that an event with the selected magnitude and distance will occur. As a result, one is not able to quantitatively assess the level of conservatism in the design of a facility that is based on DSHA. In contrast, probabilistic seismic hazard analysis (PSHA) considers all possible magnitude earthquakes (usually above some minimum magnitude, m_o), on all significant sources, at all possible distances from the site, with consideration given to the likelihood of each combination. Therefore, using PSHA allows a potential facility to be designed for ground motion with a specified probability of exceedence. Obviously, the realism of a seismic hazard analysis (both deterministic and probabilistic) is dependant on many factors, including the assumption that the sources chosen are realistic and reasonable complete (a difficult feat in itself in that one is estimating future seismic activity not only with regard to magnitude but also location).

The focus of this chapter is only on the determination of the peak ground acceleration (PGA) hazard curve { $P(PGA \geq a)$ vs. PGA }, and not design response spectra. Depending on how one proceeds, the hazard curve may be used to select a peak ground acceleration with a specified probability of exceedence, to which a fixed-shape spectrum can be scaled and anchored. Chapter 6 discusses different approaches used for determining design spectra. Outlined below are: the basic steps involved in PSHA; a description of the use of logic trees as a explicit means of documenting and quantifying uncertainty; and also a discussion of the assumptions inherent in PSHA. Example 5.1

illustrates the steps involved in a PSHA using the same fictitious site as Example 4.1 (DSHA).

5.2 Steps involved in PSHA

In general, PSHA involves 4 basic steps: identification of sources; establishment of recurrence relationships, magnitude distribution and average rate of occurrence for each source; selection of attenuation relationship; and finally, the computation of the site hazard curve (see Figure 5.1). Uncertainty is inherent in each of these steps. For example, the length or size used to model an identified source is only a best estimate, therefore the above steps may be repeated several times using a number of different source models, attenuation expressions, etc. [National Research Council, 1988; Reiter, 1990]. The formal treatment of this uncertainty warrants its own section (Section 5.3), and therefore will not be discussed in this section. Each of the four steps will be discussed in sequential order.

5.2.1 Step 1: Identification of sources

When a prospective site for a facility is being reviewed, all seismic sources that can produce damaging ground motion at the site need to be defined. The identification of seismic source zones is based upon the interpretation of geological, geophysical, and seismological data. The exact procedures used in the interpretation of these data is beyond the scope of this report. What is presented is a brief discussion of some of the considerations involved in the identification process.

Although sources can be represented by points, lines, and areas, most are defined as areas (or zones) because of the preciseness of a point or line may not properly depict the knowledge (or lack of knowledge) of the earthquake mechanism. The length of line sources and the size of zones may vary, but each designated source is typically assumed to have uniform earthquake potential. This means that a given magnitude event

is equally likely to occur anywhere on or within a source [National Research Council, 1988]. If a line source is used to represent a well defined fault, but a portion of the fault is considerably more active than the rest, then enough source lines (within reason) should be used to properly define the fault.

Once the sources are defined, the site-to-source distance distributions can be established. As is shown in Example 5.1, the distance distribution for a given source does not have to be of closed mathematical form, but can be an array of numbers representing the distance from the site to the segments or sub-areas of a discretized source.

5.2.2 Step 2: Recurrence relationships, magnitude distributions, and average occurrence rates

The second step involved in a PSHA is the establishment of earthquake recurrence relationships, magnitude distribution, and average occurrence rates. A recurrence model specifies the relative number of earthquakes of different magnitude levels. In most cases, earthquake recurrence is expressed by the Gutenburg-Richter b-line: $\log N = a - bM$, where M = magnitude; N = expected (or average) number of earthquakes of magnitude greater than or equal M; a and b are constants for a given source. This relationship plots as a straight line with a y-intercept of "a" and slope of "b", hence the name b-line [Richter, 1958]. Multiple values of a and b can be used to represent different portions of the magnitude scale of a given source. The line(s) can be derived from regression analysis of either recorded data or a combination of recorded and geologic data, with the latter usually resulting in multi-sloped b-lines. In most cases the recurrence expression is presented in its normalized form (i.e., per unit time, per unit distance/area). It should be noted that even though the b-line can be used to compute the average occurrence rate of earthquakes, it does not address the time distribution of the events. (Section 5.2.4 discusses forecasting models which are used to correlate events

in space and time.)

Use of the Gutenberg-Richter relation implies that magnitudes are exponentially distributed [Cornell, 1968]. The magnitude probability density function is typically expressed as:

$$f(M) = c\,\beta\,e^{-\beta(M-m_o)}\ ,\quad where\quad c = \frac{1}{1 - e^{-\beta(m_{max}-m_o)}}\ ,$$

where

f(M)	=	magnitude probability density function,
β	=	b ln(10), (b = slope of b-line),
M	=	magnitude, and
m_o & m_{max}	=	the lower and upper magnitude limits, respectively.

A plot of this function is shown in Example 5.1. As with the distance distribution, the magnitude distribution can be discretized, with the center value of the each interval being used in the attenuation expression. As will be seen in the example, even for simple problems, a large number of computations are required in a PSHA. As a result, computers are normally employed; discretization is conducive of computer code solutions, even for functions where the closed mathematical form is known.

Given the occurrence of an earthquake, the probability that its magnitude and distance fall in the respective intervals needs to be determined. If the lengths or areas of each segment or sub-area for a given discretized source are equal, then there is an equal probability that an earthquake will occur on any of the segments or sub-areas. Therefore, the probability that an earthquake will occur at any one of the discretized source to site distance array values is simply 1/(the number of intervals). Given the occurrence of an earthquake, the probability that its magnitude falls in the i^{th} magnitude

interval is approximated by multiplying the magnitude probability density function evaluated at the center magnitude for that interval (M_i) by the range of the interval (ΔM), or:

$$P(M_i - \frac{\Delta M}{2} \leq M \leq M_i + \frac{\Delta M}{2}) \approx f(M_i)\,\Delta M \quad .$$

The lower limit magnitude (m_o) used in a PSHA was at first thought by the earthquake community to be inconsequential, but it was later discovered that this is not the case. In selecting m_o, a sensitivity study should be conducted to determine how much influence it has on the results [Reiter, 1990]. A Body Wave magnitude (m_b) of 5.0 is a commonly used lower bound value. Usually, the level of ground motion associated with earthquakes of this magnitude cause little damage to engineered structures.

The choice of magnitude for the maximum credible earthquake (m_{max}) has a much greater influence on the results than m_o, and varies from zone to zone. Because the earthquake database in the United States only extends back a couple of hundred years, the maximum historic earthquake for a region or source is usually used as a minimum value for m_{max}. Geologic investigations are also used to determine m_{max}. For example, correlations exist between surface fault length and maximum possible earthquake. Also, trenching a fault may determine the amount of slip and provide a clue as to the associated size of past events [Wells, 1994]. Another method presented by Nuttli and Herrmann, [Nuttli, 1978], defined the maximum earthquake for zones in the central United States by extending the associated b-lines to the 1000-year recurrence interval.

The average occurrence rate (ν) of a source is defined as the average number of events between m_o and m_{max}, per unit time. The average occurrence rate is related to the normalized recurrence expression (b-line) and the size of the source by the following expression:

$$\nu = [N(m_o) - N(m_{max})] \cdot L,$$

where $N(m_o)$ and $N(m_{max})$ are the average number of earthquakes (per unit time, per unit size) of magnitudes equal to or greater than m_o and m_{max}, respectively. L equals the size of the source.

5.2.3 Step 3: Ground motion estimation

Once the source(s) are identified, and the recurrence relationship(s) with the corresponding values of m_o and m_{max} are established, an attenuation expression needs to be selected to estimate the ground motion. As noted in Chapter 3, numerous attenuation relationships exist for various source mechanisms and geologic conditions; one appropriate for the given conditions needs to be selected.

Given the occurrence of an earthquake, the probability that the site PGA will exceed an acceleration (acc) of interest needs to be determined for every combination of discretized magnitude and distance for each identified source or stated in mathematical notation: $P(PGA > acc \mid EQ: R_j, M_i)$. Note that the vertical line and subsequent symbols read "given the occurrence of an earthquake at distance R_j of magnitude M_i." Usually, the uncertainty in an attenuation expression (resulting from the scatter in the data from which it is derived) is assumed to be log-normally distributed. This assumption provides a means of quantifying the probability that given the occurrence of an earthquake of magnitude M at distance R the PGA is above (or below) an acceleration level of interest. The inclusion of this uncertainty in the analysis requires a large computational effort, but must be accounted for if a true PSHA is to be conducted. Also note that there is uncertainty resulting from the choice of attenuation relationship used. This uncertainty can be formally treated as a node in the logic tree.

5.2.4 Step 4: Construction of the hazard curve

A hazard curve combines all of the above information into one plot. The distance and magnitude distributions and ground motion probability expression for a given source are combined to

produce a statement of the probability that given the occurrence of a seismic event with a magnitude of interest anywhere on the k^{th} source, the site PGA will exceed an acceleration of interest or

$$P_k(PGA > acc \mid EQ_k) = \iint P(PGA > acc \mid EQ_k: M, R) f(M) f(R) \, dMdR \, .$$

Restated in summation notation which is applicable to the discretized distributions:

$$P_k(PGA > acc \mid EQ_k) = \sum_j \sum_i P(PGA > acc \mid EQ_k: M_i, R_j) \, f(M_i) \Delta M \, f(R_j)$$

Note that the above expression is the probability that the site PGA will exceed an acceleration of interest *given* the occurrence of an earthquake, and does not take into account the probability that an earthquake will occur.

A forecasting model needs to be selected to express the occurrence probability of future seismic events (i.e, correlation of events in space and time). Forecasting models are generally based on the theory of stochastic (or random) processes and not on the extrapolation of past data, but may employ data for the evaluation of parameters (e.g., ν, the average occurrence rate). The most widely used model is the homogeneous Poisson model [Tri-Service manual]. Some of the assumptions required in order to use this model are discussed in Section 5.4. Other proposed models include the renewal, and clustering models. It is beyond the scope of this report to describe the different types of models; mention is made only to make the reader aware that the Poisson model is not the only one that can be used.

The Poisson model of occurrence can be written as:

$$P(n,t) = \frac{(\nu t)^n e^{-\nu t}}{n!} ,$$

where P(n,t) is the probability of having exactly n events in a future time period t, and ν is the average occurrence rate. This expression reduces to P(0,1) = exp(-ν) for the probability that no events will occur in a one year time period. Therefore, the probability that at least one event will occur in the year is: p = 1 - exp(-ν) [Ang, 1975]. When this expression is combined with the probability that the site PGA will exceed an acceleration of interest (given the occurrence of an earthquake), the annual probability that the site PGA will exceed an acceleration of interest (acc) resulting from the occurrence of an earthquake at the k^{th} source becomes:

$$P_k(PGA > acc) = 1 - e^{(-\nu p)_k} ,$$

where, p is P_k(PGA > acc | EQ_k). For values of $\nu p \ll 1$, the above expression is approximately:

$$P_k(PGA > acc) = (\nu p)_k ,$$

or in expanded summation form:

$$P_k(PGA > acc) = \nu_k \sum_j \sum_i P_k(PGA > acc \mid EQ_k)\ f(M_i)\,\Delta M\ f(R_j)\,\Delta R .$$

The following expression is used to combine the hazard from each source, resulting in a site hazard curve:

$$P(PGA > acc) = 1 - \prod_k (PGA < acc)_k ,$$

or:

$$P(PGA > acc) = 1 - \prod_k \{ 1 - (PGA > acc)_k \} = 1 - \prod_k (1 - P_k) ,$$

where P = exceedence probability due to all sources,

P_k = exceedence probability due to the k^{th} source, $(PGA > acc)_k$, and

$\prod$ = series product.

5.3 Logic trees and uncertainty

The logic tree is an explicit method of documenting and quantifying the uncertainty inherent in the hazard model selected. As illustrated in Figure 5.2, a logic tree allows the consideration of a variety of source definitions, recurrence relationships, m_o and m_{max}, attenuation expressions, forecasting models, etc. Each branch at the right end of the tree represents a unique seismic hazard curve for a specified set of assumptions.

All the branches that extend from nodes are assigned a weight that quantifies the likelihood of that alternative being correct; the sum of all the weights attached to a node is unity. The assignment of the weights is a formalized method of documenting subjective inputs. The product of all the weights of the branches associated with a hazard model expresses the confidence in the associated hazard curve. From the family of hazard curves associated with the various combinations of assumptions, the mean, median, and 84^{th} percentile hazard curves can be calculated [National Research Council, 1988].

5.4 Assumptions inherent in PSHA

Anytime nature is modeled mathematically simplifying assumptions have to be made. As a result, the validity of a mathematical model is limited to scenarios where the assumptions are reasonable. The use of any engineering procedures without an understanding of the associated assumptions may lead to undesirable results; PSHA is not an exception. The following discussion points out some of the assumptions involved in PSHA.

When conducting a PSHA, assumptions are inherent in the selection of both the magnitude recurrence relationship and the

earthquake occurrence forecasting model. Although the selection of these two models is distinct, there are some over lapping of assumptions between them. The recurrence model is discussed first.

5.4.1 The Gutenberg-Richter b-line

The Gutenberg-Richter b-line is the most commonly used recurrence model. The b-line provides information concerning the magnitude distribution, given the occurrence of an event, and the average occurrence rate (ν) of earthquakes for a given region. However, the b-line does not provide information concerning the time distribution of events. For example, if the average occurrence rate of earthquakes for a given region is computed to be 12 per year, no information is provided as to whether the time distribution of the events is constant (e.g., one per month, year in, year out) or clustered (e.g., five the first month, seven the second month, and zero in the remaining ten months, or none for five years then a swarm). The assumed time distribution is inherent in the selected forecasting model, which is the topic of Section 5.4.2.

A direct comparison cannot be made among b-lines proposed by different studies even for the same region because each is sensitive to both the size of the area used to model the source, and the time interval from which the analyzed data was recorded. The b-line's sensitivity to the size of the area used to model the source is discussed first. One inherent assumption in selecting the size of an area used to model a source zone is that it be of uniform earthquake potential. Therefore, as the size of an area model increases, higher activity portions of the zone are "diluted" by lower activity portions, but in computing the seismic hazard of a site, it is assumed earthquakes only can occur in areas identified as sources. As a result, a small area with a characteristically more active b-line may present an equal hazard as that of a large area with a characteristically less active b-line. The resulting hazard curves of PSHA using

different area sizes would have to be compared to determine how sensitive the PGA is to these changes. The uncertainty in the selection of an appropriate sized model can be incorporated as a node on the logic tree, but the assigned confidence in each model is a subjective input.

The time interval from which the analyzed records are taken for use in the construction of the b-line should be as large as possible, but in the United States the historic database only extends back a couple of hundred years. When a small region or individual fault is examined, the time interval is generally much shorter, with few (if any) large events having occurred. Various methods have been proposed to make-up for the insufficient amount of historical data. In some cases, the slope and y-intercept of the b-line is determined from small magnitude events and simply extended as a straight line for larger magnitudes. Also, geologic evidence and slip rate of the fault often are used to complement the database. The assumptions inherent in extending the b-line or using geologic data have been questioned by some seismologists [Krinitzsky, 1993a]. A detailed discussion of the concerns in employing either of these approaches is beyond the scope of this report, but the reader should be aware that no one method of filling the gap resulting from an insufficient amount of data is universally accepted.

5.4.2 Poisson forecasting model

Assumptions also are involved in the selection of a probabilistic earthquake forecasting model. The Poisson model is the most commonly used forecasting model, but others such as clustering and renewal also may be employed. Two common assumptions in using the Poisson model are the constant-in-time average occurrence rate (ν) of earthquakes, and the "memory-less" behavior of occurrences. The use of a constant occurrence rate becomes unreasonable when determining the hazard for small time intervals relative to the observed clustering return period

of events. As the time interval of the analysis increases the use of a constant-in-time ν becomes more reasonable. Most structures have a useful life of 50 years or more; therefore, the use of the constant-in-time ν is typically a valid assumption. (Note: a time-varying ν may be employed, but the computational difficultly increases.)

The second assumption inherent in the use of a Poisson model is the memory-less behavior of occurrences of earthquakes at a given source. This assumption is not consistent with elastic rebound theory, which implies that a zone of recent past activity is less likely to be a source of the next earthquake than a previously active zone which has been relatively quiet for some time [Cornell, 1968]. It has been shown that the memory-less assumption is inappropriate only if the elapsed time between significant events exceeds the average recurrence time of such events [Cornell, 1988]. For example, if the average recurrence time of magnitude 8 earthquakes for a given source equals 100 years, but the last time an event of this size occurred was 150 years ago, then the memory-less assumption is inappropriate. As with time-varying ν, a forecasting model that incorporates memory may be employed, but the computational difficultly increases.

5.5 Description of Example 5.1

The same fictitious site used in Example 4.1 (DSHA) is reanalyzed using probabilistic procedures in Example 5.1. In this example, the two uniform earthquake potential sources are defined and the associated recurrence relationships given (i.e., uniform earthquake potential source: the magnitude recurrence relationship and earthquake forecasting model for all regions of a given source are the same). The steps involved in determining the hazard curve of the line source are presented in detail. Many of the calculations associated with the uncertainty of the given attenuation expression in Step 3 are repetitive and can be skipped, but all are shown for completeness. Little would be

gained by the presentation of an equally detailed analysis of the area source, therefore, only the unique features and the results are shown for this source. Also shown are the calculations involved in combining the hazard curves for the two sources and the resulting site hazard curve.

Figure 5.3 shows a plan view of the site and its orientation to the sources. This figure also shows how the sources are discretized into segments and sub-areas. In a hazard analysis of an actual site, the sources would be discretized into smaller intervals. The attenuation expression used in this example is Boore, Joyner, and Fumal (1993), which was introduced in Chapter 3. It should be noted that the site-to-source distances shown in Figure 5.3 are not necessarily the appropriate measurements defined for use with this attenuation expression, but they are used for pedagogical purposes.

> Note: the site-to-source distance defined for used with the Boore, Joyner and Fumal (1993) attenuation expression is the shortest distance from the site of interest to the point on the earth's surface directly over the fault rupture. Hence, the below grade orientations of the sources are required in order for the appropriate site-to-source distances to be determined. In cases where an area source model is used because a fault trace can not be identified, often the source is assumed to have a vertical below grade orientation.

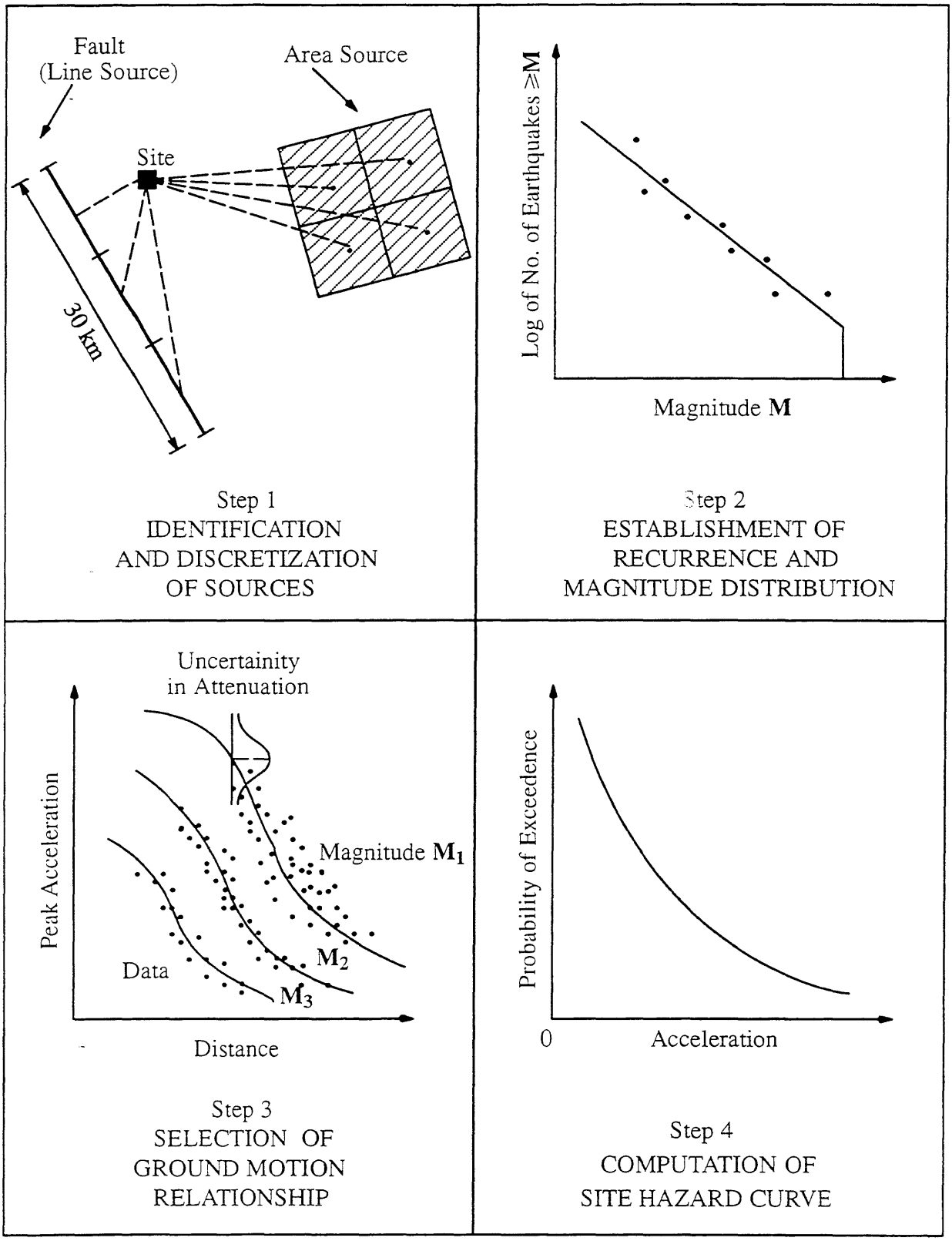

Figure 5.1 Basic steps of probabilistic seismic hazard analysis (after Reiter,1990).

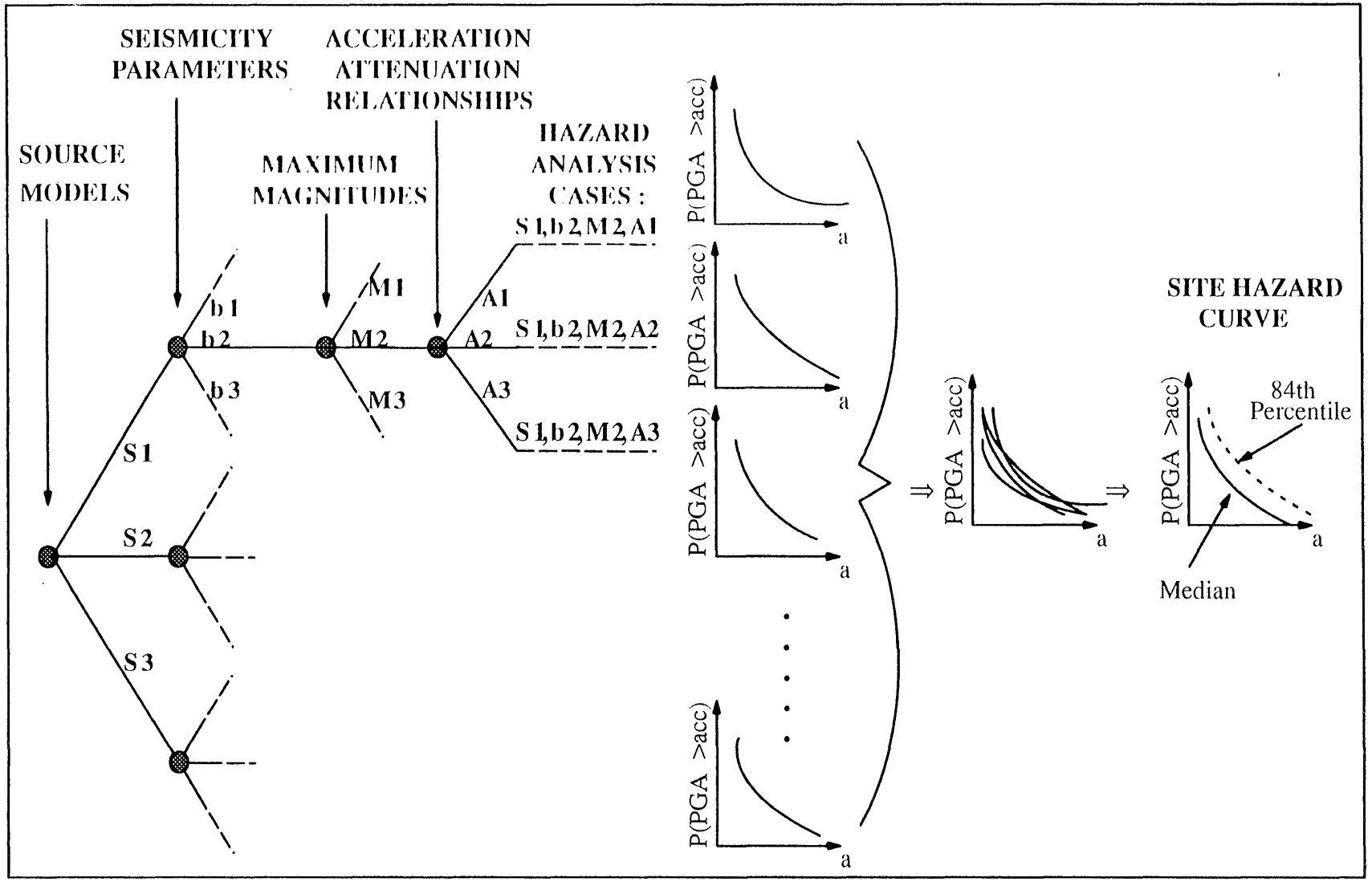

Figure 5.2 Example of logic tree format used to represent uncertainty in hazard analysis input. Each branch has an assigned weight (not shown); the sum of weights on all of the branches attached to a single node equals unity (after National Research Council, 1988).

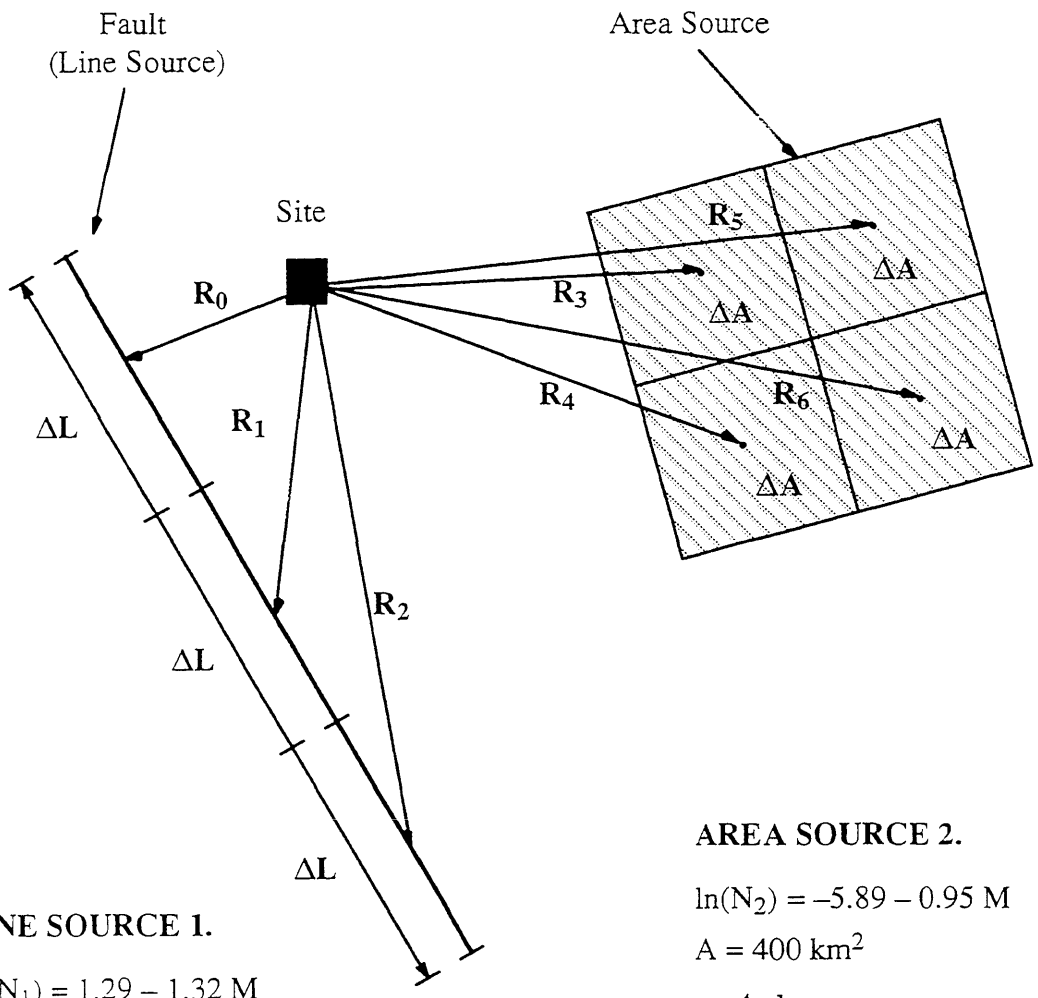

LINE SOURCE 1.

$\ln(N_1) = 1.29 - 1.32\ M$

L = 30 km

n = 3 elements

ΔL = 10 km

R_0 = 15 km

R_1 = 18 km

R_2 = 24 km

$m_{max} = 7.5$

$m_0 = 5.0$

AREA SOURCE 2.

$\ln(N_2) = -5.89 - 0.95\ M$

A = 400 km^2

n= 4 elements

ΔA = 100 km^2

R_3 = 22 km

R_4 = 28 km

R_5 = 32 km

R_6 = 37 km

$m_{max} = 6.5$

$m_0 = 5.0$

Figure 5.3 PSHA example (after Tri-Service manual, 1986).

Below is a detailed description of the hazard analysis of the line source. Only the unique features and results of the area source analysis are shown. Also, the steps involved in combining the results from both sources into a single site hazard curve are shown.

STEP 1: Indentification of sources: A well defined fault is modeled as a 30km line source. The line source is divided into three 10 km segments [Tri-Service manual].

Site-to-Source Distance Distribution:

The distance from the site to the center of each of the 3 segments:

$R_0 := 15km$

$R_1 := 18km$

$R_2 := 24km$

Because the length and recurrence relationship are the same for each segment, given that an earthquake occurs on the line source, there is a one third probability it occurred on any given segment.

$$f(R)\cdot\Delta R := \frac{1}{3}$$

STEP 2: Recurrence relationship, magnitude distribution and average rate of occurrence: Earthquake recurrence is expressed by the Gutenberg-Richter b-line.
Note: the b-line may be expressed in log (base 10) or natural log.

Recurrence Relationship:
(for entire line source)

$\ln N_1 := a_1 - b_1\cdot M$ where $a_1 := 1.29$ $b_1 := 1.32$

or

$$N_1 := e^{(1.29 - 1.32\cdot M)}$$

Example 5.1 Probabilistic seismic hazard analysis (PSHA).

Average number of earthquakes of magnitude M or greater (per year, per km)

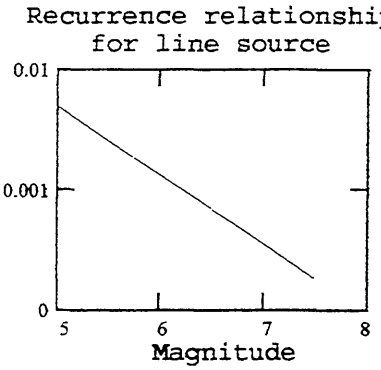

Magnitude Distribution:

The use of the b-line as a recurrence relationship implies an exponential magnitude distribution. The following magnitude limits are used in evaluating the seismic hazard of the line source:

$$m_o := 5.0 \qquad m_{max} := 7.5$$

Magnitude probability density function: $f_1(M) := c_1 \cdot \beta_1 \cdot e^{-\beta_1 (M - m_o)}$

Because the b-line is expressed in natural log form $\beta_1 = b_1$. If the b-line were expressed in log (base 10) form then $\beta_1 := b_1 \cdot \ln(10)$

Note that the area under the plot of the magnitude probability density function (below) must eqaul 1.0. Therefore, as a result of the imposed magnitude limits, constant c_1 is required. If there were no magnitude limits then $c_1 = 1.0$.

$$c_1 := \frac{1}{1 - e^{-\beta_1 \cdot (m_{max} - m_o)}}$$

$$c_1 = 1.038$$

$$f_1(M) := 1.038 \cdot 1.32 \cdot e^{-1.32 \cdot (M - 5)}$$

$$f_1(M) := 1.37 \cdot e^{-1.32 \cdot (M - 5)}$$

Example 5.1 (continued).

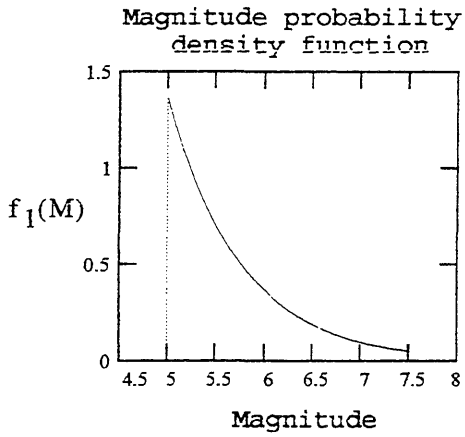

The magnitude range is divided into subintervals with increments of 0.5 M. The center magnitude of each subinterval is then calculated for subsequent use.

$$\Delta M := 0.5$$

$5.0 < M < 5.5$	$M_{mid_0} := 5.25$
$5.5 < M < 6.0$	$M_{mid_1} := 5.75$
$6.0 < M < 6.5$	$M_{mid_2} := 6.25$
$6.5 < M < 7.0$	$M_{mid_3} := 6.75$
$7.0 < M < 7.5$	$M_{mid_4} := 7.25$

Given that an earthquake occurs, the probability that its magnitude falls in a given subinterval is approximated by evaluating the magnitude probability density function at the center value of the subinterval and multipling the result by the interval increment:

$$P\left(M_{mid_i} - \frac{\Delta M}{2} < M < M_{mid_i} + \frac{\Delta M}{2} \right) = f_1\left(M_{mid_i}\right) \cdot \Delta M$$

Example 5.1 (continued).

$$P(5.0<M<5.5|EQ) = f_1\left(M_{mid_0}\right)\cdot\Delta M$$

$$= f_1(5.25)\cdot 0.5$$

$$= 1.37\cdot e^{-1.37\cdot(5.25-5)}\cdot 0.5$$

$$= 0.985\cdot 0.5$$

$$= 0.493$$

$$P(5.5<M<6.0|EQ) = f_1\left(M_{mid_1}\right)\cdot\Delta M = 0.255$$

$$P(6.0<M<6.5|EQ) = f_1\left(M_{mid_2}\right)\cdot\Delta M = 0.132$$

$$P(6.5<M<7.0|EQ) = f_1\left(M_{mid_3}\right)\cdot\Delta M = 0.068$$

$$P(7.0<M<7.5|EQ) = f_1\left(M_{mid_4}\right)\cdot\Delta M = 0.035$$

where $\sum_i f_1\left(M_{mid_i}\right)\cdot\Delta M = 1.0$ (approximately due to discretization error)

The approximated probability that an earthquake's magnitude falls in a specified magnitude subinterval, (given the occurrence of an earthquake), is represented in the following plot as the area bounded by the rectangle corresponding to the specified subinterval.

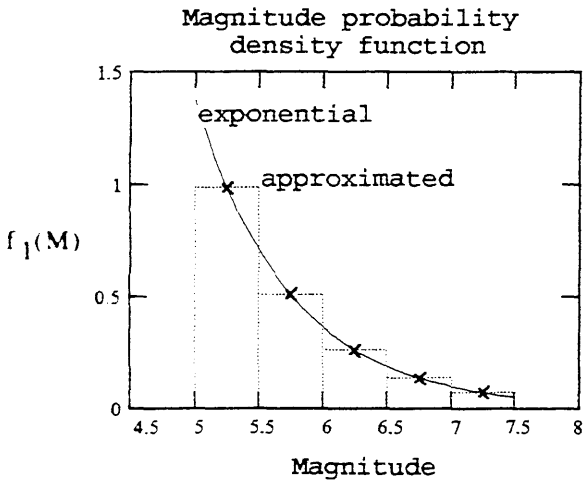

Example 5.1 (continued).

Average Occurrence Rate:

The average occurrence rate of earthquakes (per year) with magnitudes of interest (i.e., 5<M<7.5) for the entire 30km line source is,

$$\nu_1 := \left(N_1(5) - N_1(7.5)\right) \cdot L \ ,$$

Where N1(5) and N1(7.5) are the average number of earthquakes per year of M>5 and M>7.5, respectively.

$$N_1(5) := e^{(1.29 - 1.32 \cdot 5)} = 0.005$$

$$N_1(5) := e^{(1.29 - 1.32 \cdot 7.5)} = 0.0002$$

$$L := 30$$

$$\nu_1 := (0.005 - 0.0002) \cdot 30$$

$$\nu_1 = 0.143$$

STEP 3: Ground motion estimation: The ground motion (or peak ground acceleration) is estimated through an attenuation function. The Boore, Joyner and Fumal (1993) expression is used with the coefficients corresponding to the largest horizontal component of the PGA (for site class A) [Boore, 1993].

Mean/Median log(PGA):

$$\text{logPGA} := -0.038 + 0.216 \cdot (\text{Mmid} - 6) - 0.777 \cdot \log\left[\sqrt{(R)^2 + 30.03}\right]$$

$$\sigma_{\text{logPGA}} := 0.205$$

Median PGA:

$$\text{PGA} := 10^{\text{logPGA}}$$

Example 5.1 (continued).

The following are plots of the attenuation expression evaluated at the center magnitudes of each subinterval and varying distances. The vertical axis is peak ground acceleration (g's), and the horizontal axis is distance (km).

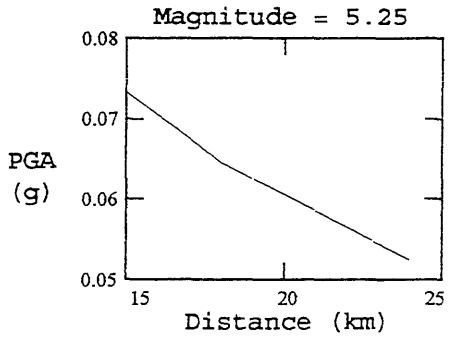

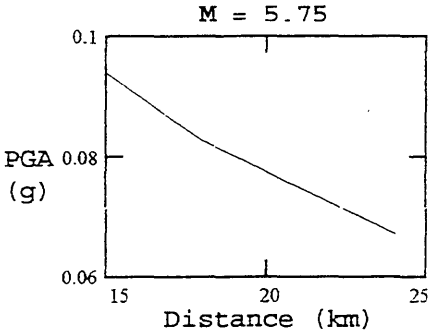

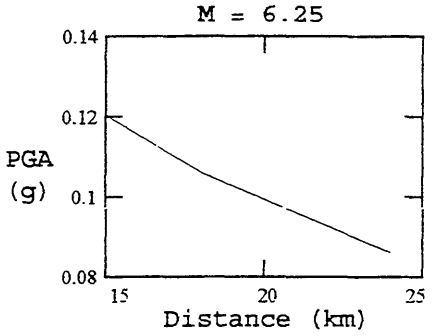

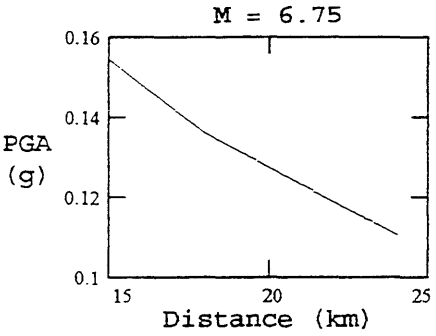

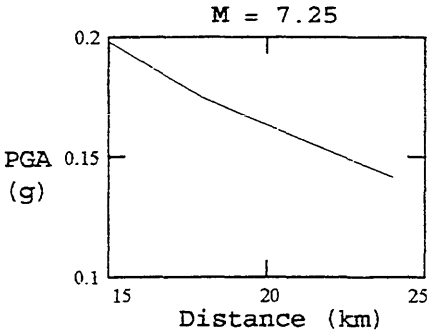

Example 5.1 (continued).

Note that the above plots do not show the inherent uncertainty associated with each line. The uncertainty is a result of the scatter in the data used in the derivation of the attenuation expression which is typically assumed to be log-normally distributed. Based on this assumption that the uncertainty of the PGA is log-normally distributed, the uncertainty of "logPGA" is normally distributed. For normal distributions the mean and median values are equal, but not for log-normal distributions. This uncertainty is taken into account by using the Φ function; the steps involved in the use of the Φ function are outlined on the next page.

Determination of Median PGA for M=5.25 and R=15km:

$$\text{logPGA (@M=5.25, R=15km)} = -0.038 + 0.216\cdot(5.25 - 6) - 0.777\cdot\log\left(\sqrt{15^2 + 30.03}\right)$$

$$\text{logPGA (@M=5.25, R=15km)} = -1.135$$

$$\text{PGA (@M=5.25, R=15km)} = 10^{-1.135}$$

$$\text{PGA (@M=5.25, R=15km)} = 0.073\ g$$

Repeat the above computations for PGA for every combination of magnitude and distance; the results are displayed in the tables below. Each column corresponds to a fixed site-to-source distance, and increasing magnitude (i.e., center magnitudes of the subintervals). Note that the PGA solved for above (i.e., PGA = 0.073g) is the in the first row and first column in the "Median PGA" table (next page).

Mean/Median logPGA:

	R=15km	R=18km	R=24km
M=5.25	-1.135	-1.190	-1.281
M=5.75	-1.027	-1.082	-1.173
M=6.25	-0.919	-0.974	-1.065
M=6.75	-0.818	-0.866	-0.957
M=7.25	-0.703	-0.758	-0.849

Example 5.1 (continued).

Median PGA (g):

	R=15km	R=18km	R=24km
M=5.25	0.073	0.065	0.052
M=5.75	0.094	0.083	0.067
M=6.25	0.121	0.106	0.086
M=6.75	0.155	0.136	0.110
M=7.25	0.198	0.174	0.142

The accelerations of interest (acc) that will examined in this example range from 0.05g to 0.65g; an increment of 0.05g is used.

$acc_0 := 0.05g$

$acc_1 := 0.10g$

$acc_2 := 0.15g$

.

.

.

.

$acc_{12} := 0.65g$

The probabilities that the PGA will exceed the accelerations of interest (acc = 0.05 to 0.65g) for every combination of magnitude and distance need to be determined.

Use the Φ function and associated table of standard normal probability [Ang, 1975] to determine the probability that the PGA will exceed an acceleration of interest (acc), given the occurrence of an earthquake of magnitude M and at distance R:

$$P(PGA < acc \mid EQ{:}R,M) = \Phi\left(\frac{\ln(acc) - \lambda}{\zeta}\right)$$

where $\lambda = E[\ln(PGA)]$, and

Note: $E[\ln(PGA)]$ = mean value of $\ln(PGA)$

$\zeta = \sigma_{\ln PGA}$.

Example 5.1 (continued).

Because the Boore, Joyner, and Fumal (1993) attenuation relationship is expressed in "log" (base 10) form as opposed to "ln" form, the following form of the PHI function is used to facilitate calculations. (Note: the factor of 2.303cancels out from both the numerator and demonimator.)

$$\ln(acc) = 2.303 \log(acc),$$

$$\lambda = E[\ln(PGA)] = 2.303\, E[\log(PGA)], \text{ and}$$

$$\zeta = \sigma_{\ln PGA} = 2.303 \cdot \sigma_{\log PGA}$$

$$P(PGA < acc \mid EQ{:}R,M) = \Phi\left(\frac{\ln(acc) - \lambda}{\zeta}\right)$$

$$= \Phi\left(\frac{2.303 \cdot \log(acc) - 2.303 \cdot \log PGA}{\sigma_{\log PGA}}\right)$$

$$= \Phi\left(\frac{\log(acc) - \log PGA}{\sigma_{\log PGA}}\right)$$

$$P(PGA > acc \mid EQ{:}R,M) = 1 - \Phi\left(\frac{\log(acc) - \log PGA}{\sigma_{\log PGA}}\right)$$

$$P(PGA > 0.05g \mid EQ{:}R=15,\ M=5.25) = 1 - \Phi\left(\frac{\log(0.05) - \log(0.073)}{0.205}\right)$$

$$= 1 - \Phi\left(\frac{-1.301 + 1.135}{0.205}\right)$$

$$= 1 - \Phi(-0.802)$$

$$= \Phi(0.8017)$$

use table of standard normal distribution [Ang, 1975]

$$= 0.791$$

Example 5.1 (continued).

Repeat the above computations for the probability that, given the occurrence of an earthquake at every combination of discretized site-to-source distance (R) and discretized magnitude (M), the PGA will exceed a fixed discretized acceleration of intererest (acc); the results are displayed in the tables below. Note that the value in the first column of the first row of the first table (i.e., 0.791) was computed above.

P(PGA > 0.05g | EQ: R,M)

	R=15km	R=18km	R=24km
M=5.25	0.791	0.705	0.539
M=5.75	0.909	0.857	0.734
M=6.25	0.969	0.945	0.875
M=6.75	0.992	0.983	0.953
M=7.25	0.998	0.996	0.986

P(PGA > 0.10g | EQ: R,M)

	R=15km	R=18km	R=24km
M=5.25	0.255	0.177	0.085
M=5.75	0.448	0.344	0.199
M=6.25	0.654	0.550	0.376
M=6.75	0.822	0.743	0.583
M=7.25	0.926	0.881	0.769

Example 5.1 (continued).

P(PGA > 0.15g | EQ: R,M)

	R=15km	R=18km	R=24km
M=5.25	0.065	0.037	0.013
M=5.75	0.161	0.104	0.044
M=6.25	0.321	0.232	0.120
M=6.75	0.525	0.418	0.258
M=7.25	0.722	0.626	0.451

P(PGA > 0.20g | EQ: R,M)

	R=15km	R=18km	R=24km
M=5.25	0.017	0.008	0.002
M=5.75	0.055	0.031	0.010
M=6.25	0.142	0.090	0.037
M=6.75	0.292	0.207	0.104
M=7.25	0.492	0.386	0.232

P(PGA > 0.25g | EQ: R,M)

	R=15km	R=18km	R=24km
M=5.25	0.005	0.002	4.63x10^-4
M=5.75	0.019	0.010	0.003
M=6.25	0.061	0.035	0.012
M=6.75	0.154	0.099	0.042
M=7.25	0.311	0.223	0.114

Example 5.1 (continued).

P(PGA > 0.30g | EQ: R,M)

	R=15km	R=18km	R=24km
M=5.25	0.001	5.66x10^-4	1.09x10^-4
M=5.75	0.007	0.003	7.59x10^-4
M=6.25	0.027	0.014	0.004
M=6.75	0.080	0.047	0.017
M=7.25	0.190	0.125	0.056

P(PGA > 0.35g | EQ: R,M)

	R=15km	R=18km	R=24km
M=5.25	4.63x10^-4	1.70x10^-4	2.85x10^-5
M=5.75	0.003	0.001	2.35x10^-4
M=6.25	0.012	0.006	0.001
M=6.75	0.042	0.023	0.007
M=7.25	0.114	0.070	0.028

P(PGA > 0.40g | EQ: R,M)

	R=15km	R=18km	R=24km
M=5.25	1.62x10^-4	5.55x10^-5	8.25x10^-6
M=5.75	0.001	4.21x10^-4	7.82x10^-5
M=6.25	0.006	0.002	5.69x10^-4
M=6.75	0.022	0.011	0.003
M=7.25	0.068	0.039	0.014

Example 5.1 (continued).

P(PGA > 0.45g | EQ: R,M)

	R=15km	R=18km	R=24km
M=5.25	6.03x10^-5	1.94x10^-5	2.59x10^-6
M=5.75	4.54x10^-4	1.67x10^-4	2.79x10^-5
M=6.25	0.003	0.001	2.30x10^-4
M=6.75	0.012	0.006	0.001
M=7.25	0.041	0.022	0.007

P(PGA > 0.50g | EQ: R,M)

	R=15km	R=18km	R=24km
M=5.25	2.37x10^-5	7.19x10^-6	8.75x10^-7
M=5.75	1.99x10^-4	6.92x10^-5	1.05x10^-5
M=6.25	0.001	5.11x10^-4	9.70x10^-5
M=6.75	0.006	0.003	6.88x10^-4
M=7.25	0.025	0.013	0.004

P(PGA > 0.55g | EQ: R,M)

	R=15km	R=18km	R=24km
M=5.25	9.78x10^-6	2.82x10^-6	3.14x10^-7
M=5.75	9.09x10^-5	3.00x10^-5	4.19x10^-6
M=6.25	6.50x10^-4	2.45x10^-4	4.27x10^-5
M=6.75	0.004	0.002	3.35x10^-4
M=7.25	0.015	0.007	0.002

Example 5.1 (continued).

P(PGA > 0.60g | EQ: R,M)

	R=15km	R=18km	R=24km
M=5.25	4.21x10^-6	1.16x10^-6	1.19x10^-7
M=5.75	4.29x10^-5	1.35x10^-5	1.74x10^-6
M=6.25	3.36x10^-4	1.21x10^-4	1.95x10^-5
M=6.75	0.002	8.34x10^-4	1.68x10^-4
M=7.25	0.009	0.004	0.001

P(PGA > 0.65g | EQ: R,M)

	R=15km	R=18km	R=24km
M=5.25	1.88x10^-6	4.95x10^-7	4.75x10^-8
M=5.75	2.09x10^-5	6.30x10^-6	7.57x10^-7
M=6.25	1.78x10^-4	6.15x10^-5	9.24x10^-6
M=6.75	0.001	4.61x10^-4	8.64x10^-5
M=7.25	0.006	0.003	6.22x10^-4

STEP 4, The development of the hazard curve: All of the above probabilites are for the peak ground acceleration's exceedence of an acceleration of interest (acc) for all combinations of magnitude and distance, GIVEN the occurrence of an earthquake: P(PGA > a | EQ,M,R). In this step the probability that an earthquake will occur is taken into consideration. The occurrence of earthquakes from the line source is assumed to follow a poisson process. The Gutenberg-Richter b-line is used in this step to determine the average occurrence rate of earthquakes with magnitudes between m_o and m_{max}.

Example 5.1 (continued).

Restatement of source parameters:

Because the source is assumed to be of uniform earthquake potential and is divided into 3 segments of equal length, the probability of the occurrence of an earthquake is the same for all segments.

$$L := 30\,km$$

$$f(R)\cdot\Delta R := \frac{1}{3}$$

Restatement of Gutenberg-Richter recurrence relationship: Where N1 equals the average number of earthquakes of magnitude M or greater per year.

$$\ln(N_1) := a_1 - b_1\cdot M$$

$$N_1 := e^{1.29 - 1.32\cdot M}$$

Only earthquakes greater than mo are of interest; also, the maximum magnitude earthquake the line source is capable of generating is mmax.

$$m_o := 5.0$$

$$m_{max} := 7.5$$

Restatement of the probability that given the occurrence of an earthquake, its magnitude falls in a specified subinterval.

$$P(5.0<M<5.5\,|\,EQ) = f_1\left(M_{mid_0}\right)\cdot\Delta M := 0.493$$

$$P(5.5<M<6.0\,|\,EQ) = f_1\left(M_{mid_1}\right)\cdot\Delta M := 0.255$$

$$P(6.0<M<6.5\,|\,EQ) = f_1\left(M_{mid_2}\right)\cdot\Delta M := 0.132$$

$$P(6.5<M<7.0\,|\,EQ) = f_1\left(M_{mid_3}\right)\cdot\Delta M := 0.068$$

$$P(7.0<M<7.5\,|\,EQ) = f_1\left(M_{mid_4}\right)\cdot\Delta M := 0.035$$

Example 5.1 (continued).

The average occurence rate of earthquakes with magnitudes of interest per year for the entire source length: $\nu_1 = 0.143$

The probability of exceedence for this example is on a per year basis. $t = 1$ year

P(PGA > acc | an earthquake occurs):

$$P(PGA > acc \mid EQ) = \int_{Rmin}^{Rmax} \int_{m_o}^{m_{max}} P(PGA > acc \mid EQ{:}M,R)\ f(M)\, f(R)\, dM\, dR$$

or in summation notation:

$$P(PGA > acc \mid EQ) = \sum_{R} \sum_{M} P(PGA > acc \mid EQ{:}\ M,R)\ f(M)\cdot\Delta M\, f(R)\cdot\Delta R$$

The above probabilities are for "given the occurrence of an earthquake on the line source." A Poisson forecasting model is employed to account for the probability that an earthquake occurs.

$$P(PGA > acc) = 1 - \exp\left(-\nu_1 \cdot t \cdot p(a)\right)$$

where $p(a) = P(PGA > acc \mid EQ)$

For $\nu_1 * t * p \ll 1$, P(PGA > acc) can beapproximated by:

$$P(PGA > acc) = \nu_1 \cdot p(a)$$

Example 5.1 (continued).

acc	P(PGA>acc|EQ)	P(PGA>acc)	P(PGA>acc) approx
0.05g	0.770	0.104	0.110
0.10g	0.317	0.044	0.045
0.15g	0.123	0.017	0.018
0.20g	0.051	0.007	0.007
0.25g	0.023	0.003	0.003
0.30g	0.011	0.002	0.002
0.35g	0.005	7.70x10^-4	7.71x10^-4
0.40g	0.003	3.99x10^-4	3.99x10^-4
0.45g	0.001	2.14x10^-4	2.14x10^-4
0.50g	8.27x10^-4	1.18x10^-4	1.18x10^-4
0.55g	4.68x10^-4	6.69x10^-5	6.69x10^-5
0.60g	2.71x10^-4	3.88x10^-5	3.88x10^-5
0.65g	1.61x10^-4	2.29x10^-5	2.29x10^-5

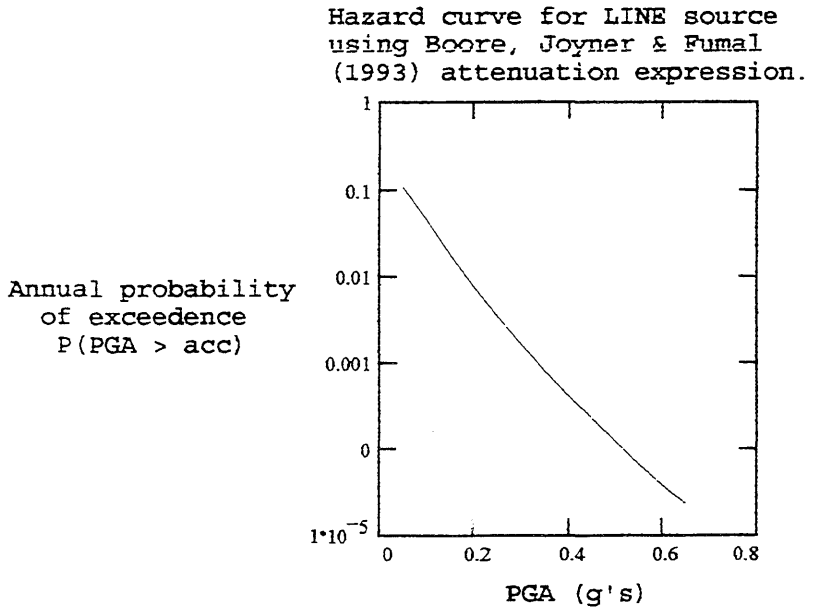

Example 5.1 (continued).

The above calculations were only for the line source, and not for the area source. Little would be gained by the inclusion of all the steps involved in hazard analysis for the area source, therefore, only the unique features and results will be presented. In this example the area source is divided into 4 equal sized sub-areas, each having the same probability that an earthquake will occur within its boundries. After the presentation of the area hazardcurve, the steps involved in combining the results from both sources into a single site hazard curve are shown.

The distance from the site to the center of each of the 4 equal sized sub-areas (km):

$R_3 := 22km$

$R_4 := 28km$

$R_5 := 32km$

$R_6 := 37km$

$f(R)\cdot\Delta R := \frac{1}{4}$

Recurrence expression: $a_2 := -5.89$ $b_2 := 0.95$

$N_2 := e^{a2 - b2\cdot M}$ $N_2 := e^{(-5.89 - 0.95M)}$

Average number of earthquakes of magnitude m or greater (per year, per km^2).

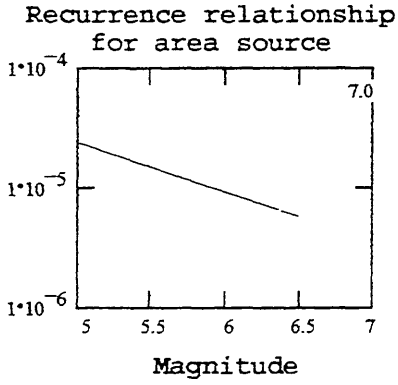

Magnitude bounds: $m_{max} := 6.5$ $m_o := 5.0$

Example 5.1 (continued).

Magnitude probability density function:

$$f_2(M) := 1.251 \cdot e^{-0.95 \cdot (M-5)}$$

$$\Delta M := 0.5$$

$P(5.0<M<5.5) = f_2(5.25) \cdot \Delta M = 0.493$

$P(5.5<M<6.0) = f_2(5.75) \cdot \Delta M = 0.307$ (approximately)

$P(6.0<M<6.5) = f_2(6.25) \cdot \Delta M = 0.191$

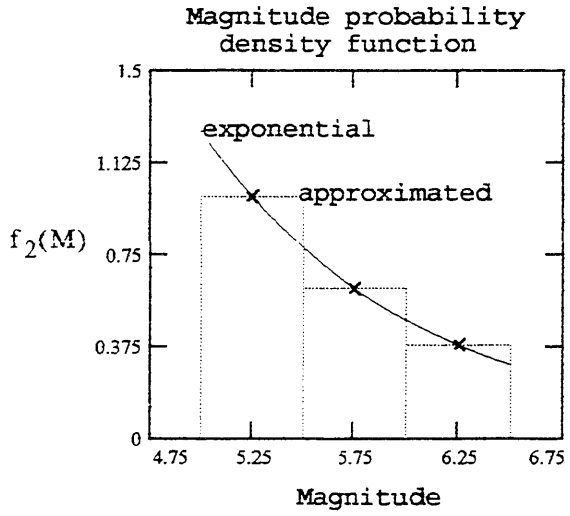

The average occurrence rate of earthquakes with magnitudes of interest for the entire 400 km^2 area source, per year.

$\nu_2 = 0.007$

Example 5.1 (continued).

The probability of exceedence P(PGA > acc) for the area source (and a restatement of the probability of exceedence for the line source):

acc	$P(PGA>acc)_1$ (line source)	$P(PGA>acc)_2$ (area source)
0.05g	0.104	0.004
0.10g	0.044	8.68x10^-4
0.15g	0.017	1.96x10^-4
0.20g	0.007	5.03x10^-5
0.25g	0.003	1.45x10^-5
0.30g	0.002	4.65x10^-6
0.35g	7.70x10^-4	1.62x10^-6
0.40g	3.99x10^-4	6.07x10^-7
0.45g	2.14x10^-4	2.42x10^-7
0.50g	1.18x10^-4	1.01x10^-7
0.55g	6.69x10^-5	4.46x10^-8
0.60g	3.88x10^-5	2.04x10^-8
0.65g	2.29x10^-5	9.71x10^-9

Hazard curve for AREA source using Boore, Joyner & Fumal (1993) attenuation expression.

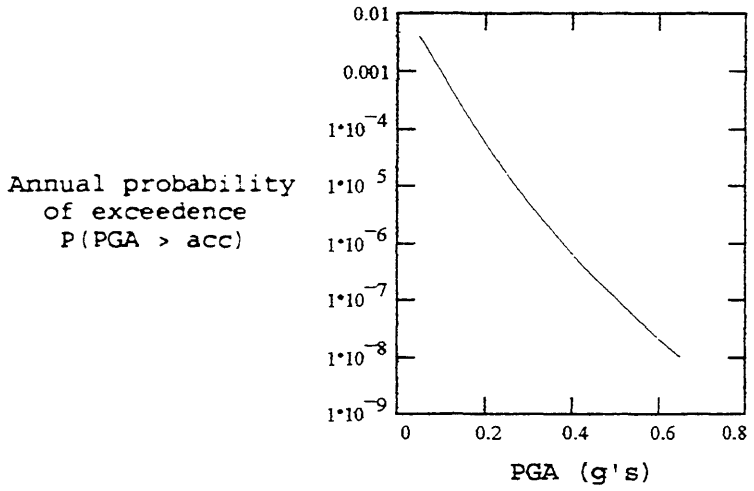

Example 5.1 (continued).

The results from the line and area sources are combined with the following expression:

$$P(PGA > acc) = 1 - \prod_{k} (PGA<acc)_k$$

OR

$$P(PGA > acc) = 1 - P(PGA<acc)_1 * P(PGA<acc)_2$$

{line source} {area source}

$$P(PGA > acc) = 1 - \{ 1 - P(PGA>acc)_1 \} * \{ 1 - P(PGA>acc)_2 \}$$

$$P(PGA > 0.05g) = 1 - (1 - 0.104)*(1 - 0.004)$$

$$= 1 - (0.896)*(0.996)$$

$$= 1 - (0.892)$$

$$= 0.108$$

Repeat the above computations for each discretized acceleration of interest value; the results are presented in the table below.

acc	P(PGA>acc)
0.05g	0.108
0.10g	0.045
0.15g	0.017
0.20g	0.007
0.25g	0.003
0.30g	0.002
0.35g	7.75x10^-4
0.40g	4.03x10^-4
0.45g	2.17x10^-4
0.50g	1.20x10^-4
0.55g	6.84x10^-5
0.60g	3.98x10^-5
0.65g	2.37x10^-5

Use linear interpolation to determine acceleration associated with a P(PGA > acc) = 0.001 .

$$PGA_{0.001} = 0.34g$$

Example 5.1 (continued).

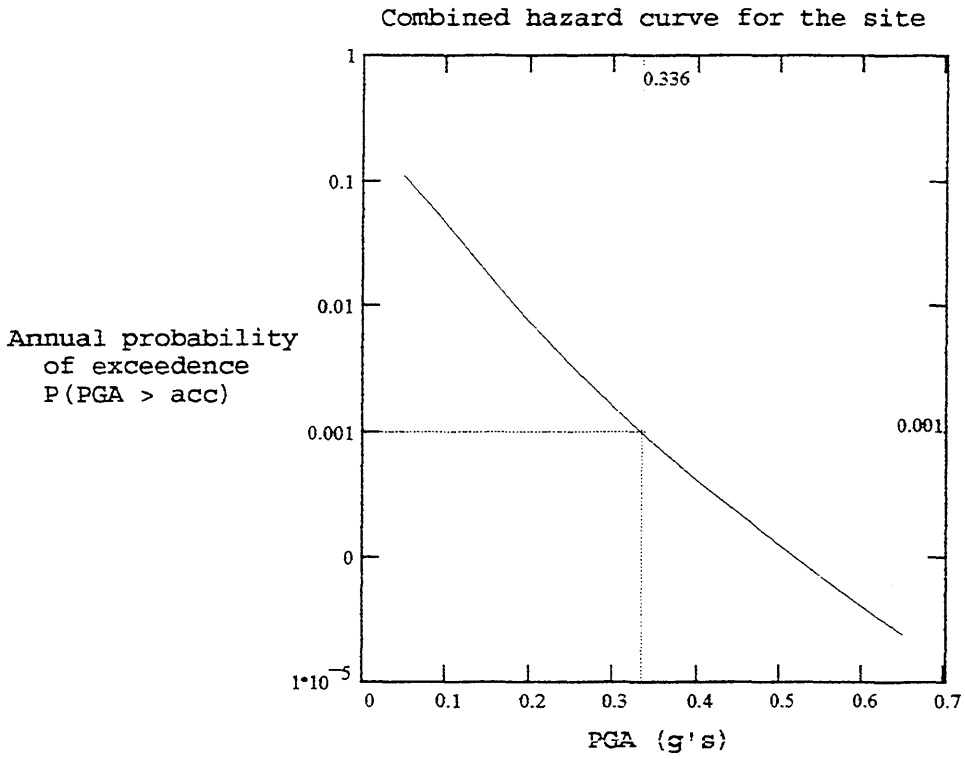

Note that the y-intercept (@PGA = 0.0g) for the above plot is approximately only 15%. At first glance the graph may seem to be in error because the ground is normally at rest, therefore the probability of exceeding 0.0g should be 100%? The plot is not wrong; the only way for the ground motion to EXCEED 0.0g is for an earthquake to occur. In this case the distance and activity of the sources result in the above hazard. Also note that the choice of the lower bound magnitude, m_o , will affect the portion of the curve corresponding to low values of PGA. In general, the lower the value of m_o used the higher the left portion of the curve will rise.

Example 5.1 (continued).

CHAPTER 6
DESIGN RESPONSE SPECTRA

6.1 Introduction

In Chapters 4 and 5, two approaches for determining the peak ground acceleration (PGA) for a site are presented, but for design purposes, a more descriptive characterization of the ground motion is required. A design response spectrum (or design spectrum) is one method of characterizing the design ground motion in a more descriptive manner that is useful in practice. A design spectrum is not a specification of a particular earthquake, but rather, a simplified curve from which the seismic resistance required in a design can be determined. Note that a design spectrum is different than response spectrum, which portray the maximum responses of single-degree-of-freedom oscillators with varying resonant frequencies to a given earthquake [Housner, 1982]. Although different, design and response spectra are related in that the former are often statistically derived from a set of the latter.

There are three general types of design spectra: scaled fixed-shape spectra, spectra obtained through spectral attenuation relations, and uniform hazard spectra [Abrahamson, 1994]. A description of each is presented below. Also, Examples 4.1 and 5.1 are continued with site design spectra being determined using several different approaches.

6.2 Scaled fixed-shape spectra

Scaled fixed-shape spectra are design spectra with standard shapes that, in general, are directly derived from the statistical analysis of real earthquake response spectra. The earthquake records and exact method of analysis used in their derivation varies depending on who and when the study was conducted. It is interesting to note that much of the early work in determining spectra shapes was related to blast loading, and then later applied to earthquakes. Commonly used fixed-

shape design spectra include the Housner spectra, the U.S. Atomic Energy Commission Regulatory Guide 1.60 spectra, the Blume spectra, and the Newmark-Hall spectra [Newmark, 1973; Newmark, 1978; Newmark, 1982]. A brief synopsis of the Newmark-Hall spectra is presented below.

Professors Nathan M. Newmark and William J. Hall, of the University of Illinois, proposed a method for scaling a fixed-shape design spectra that quickly gained in popularity. After reviewing a myriad of western United States earthquake response spectra plotted on tripartite log paper, a colleague of Newmark and Hall, Professor A. Veletsos of Rice University, concluded that most of the spectra were trapezoidal in shape. By classifying strong motion records (i.e., PGA > 0.05g) based on PGA and then normalizing the responses in the low, intermediate, and high frequency ranges by peak ground displacement (PGD), peak ground velocity (PGV), and PGA, respectively, Newmark and Hall arrived at the amplification factors--the ratio of the computed response to the maximum ground motion--at discrete frequencies. The 50^{th} (median) and 84^{th} (mean plus one standard deviation) percentile amplification factors for the three frequency ranges for each set of response spectra in a given PGA category were then computed. Also, correlations were determined among each of the three maximum ground motion parameters in the forms of ad/v^2 and v/a, where a, v, and d represent PGA, PGV, and PGD, respectively. The result of their research culminated in a simplified method of scaling a fixed-shape spectra in each of the three frequency ranges based on the design PGA and to a lesser extent, soil type. Numerous reports are available that provide an in-depth description of the evolution of research that led to this now famous spectra [Hall, 1976; Newmark, 1982; U.S. Atomic Energy Commission, 1973]. The steps involved in constructing the Newmark-Hall spectra are outlined below.

(1) Establish the expected PGA value for the design earthquake determined by either deterministic or

probabilistic procedures.

(2) Calculate the corresponding expected peak values of ground velocity and displacement using the relations

$$v = c_1 \frac{a}{g} \qquad d = c_2 \frac{v^2}{a}$$

where a, v, and d represent the design PGA, PGV, and PGD, respectively; g is the acceleration due to gravity; and constants c_1 and c_2 are selected appropriately for the known site conditions.

(3) Having established numerical values for a, v, and d, multiply them by their respective amplification factors: α_a, α_v, and α_d, corresponding to either the 50^{th} or 84^{th} percentile. Plot the results on tripartite log paper as a series of straight lines parallel to the respective axes (e.g., a line of amplitude $\alpha_d d$ should be parallel with the displacement axis).

(4) The design spectrum curve must approach the design PGA as the frequency increases. Let f_1 be the frequency on the design spectrum corresponding to the point of intersection of the lines associated with $\alpha_v v$ and $\alpha_a a$. The amplified ground acceleration ($\alpha_a a$) should approach the design PGA in a linear fashion starting at $4*f_1$ (approximately 8 Hz) and ending at approximately 33 Hz [Clough, 1993; Newmark, 1982].

Tables containing the amplification factors (α_a, α_v, and α_d) and the constant values c_1 and c_2 can be found in the referenced reports [Hall, 1976; Newmark, 1982].

The design PGA used to scale and anchor a fixed-shape spectra can be determined by either DSHA or PSHA, but one cannot assign a unique probabilistic meaning to the resulting spectrum in either case [Cornell, 1993]. This may be obvious when the spectrum is used with the PGA determined through DSHA because, as noted in Chapter 4, this PGA is not affiliated with a specified return period. Although the PGA determined through PSHA is affiliated with a specified probability of exceedence, the 50^{th} and 84^{th} percentile ranking of the design spectra are statistical and not probabilistic statements, and therefore, only provide qualitative descriptions regarding their associated

conservatism. For example, the 84th percentile ranking associated with the respective Newmark-Hall spectra only indicates that 84% of the normalized response spectra analyzed in their study fell below this design spectrum, and not that 84% of the response spectra of future earthquakes that affect a given site *will* fall below this spectra.

6.3 Attenuation relation design spectra

The use of fixed-shape spectra has advantages in its simplicity; all that is needed is the PGA for the design event and possibly the site soil conditions, but it is not without critics. Some feel that empirical evidence shows a strong correlation among spectra shape, magnitude, and distance, which is not accounted for by the use of fixed-shape spectra. An alternate method for developing design spectra whose shape is a function of both magnitude and distance is through the use of spectral attenuation relationships. As with the acceleration attenuation expressions, spectral attenuation relationships can be either empirical or theoretical in form. Both the Crouse (1991), and the Boore, Joyner and Fumal (1993) empirical acceleration attenuation expressions presented in Chapter 3 also may be used as spectral attenuation expressions when the appropriate constants are employed:

Boore, Joyner and Fumal (1993):

$$\log_{10}(S_{PV}) = b_1 + b_2(M-6) + b_3(M-6)^2 + b_4\sqrt{(R^2+h^2)} + b_5\log_{10}\{\sqrt{(R^2+h^2)}\} + b_6G_B + b_7G_C + \sigma,$$

Crouse (1991):

$$\ln(S_{PV}) = b_1 + b_2M + b_3M^2 + b_4\ln(R + b_5\exp(b_6M)) + b_7h + \sigma,$$

where S_{PV} is the pseudo spectral velocity (cm/sec); M is Moment magnitude; R is distance (km); b_1-b_7 are constants; and h is focal depth for Crouse and a constant for Boore, Joyner, and Fumal. Empirical expressions of this type are derived from

regression analysis of response spectra grouped according to magnitude and distance. This grouping is in contrast to the method employed by Newmark and Hall, who performed statistical analysis on sets of earthquake records grouped according to PGA [Cornell, 1993].

Although the Hanks and McGuire (1981) acceleration attenuation expression presented in Chapter 3 is not directly applicable for the calculation of design spectra, the theory on which it is based forms the foundation of many theoretical (or stochastic) type spectral attenuation expressions. One such expression proposed by Silva et. al, [Silva, 1989], to calculate the acceleration Fourier amplitude spectrum a(f), where f is frequency, for a point source in a homogeneous, uniform half space is:

$$a(f) = C\frac{f^2}{1+(f/f_o)^2}\frac{M_o}{R}e^{-\pi\kappa f}A(f)\,e^{\frac{-\pi fR}{\beta Q}} ,$$

where

$$f_o = 10^7\beta\sqrt[3]{\frac{\Delta\sigma}{8.5\times10^{(1.5M+16)}}} ,$$

and where the parameters can be categorized as follows:

Source parameters:	M_o	=	$10^{(1.5M\,+\,16)}$; Seismic moment,
	M	=	Moment magnitude,
	$\Delta\sigma$	=	stress parameter;
Path parameters:	Q	=	quality factor, (see Section 3.2.1);
Site parameters:	κ	=	kappa factor; accounts for damping in the shallow rock,
	A(f)	=	Amplification factor for the impedance contrast from the source to site;
Other parameters:	R	=	distance to the equivalent point source,
	β	=	shear wave velocity at the source, and
	C	=	constant.

For more information on stochastic models the reader is referred to the following papers: [Boore, 1983, 1986; Silva, 1989; and Silva, 1992]. Also, studies conducted by Professor D.V. Helmberger, of the California Institute of Technology, currently are ongoing in the derivation of time-domain based attenuation relationships.

Both empirical and theoretical spectral attenuation relationships can be used in either DSHA or PSHA, but in a different fashion than the fixed-shaped spectra. Spectra determined by spectral attenuation expressions are not scaled or anchored, but rather, spectral velocities are computed directly for a give period or frequency. For DSHA, only the distance and magnitude of the associated design event are required for computing the spectrum, but the PGA may be used in the selection of the design event (or controlling earthquake). As with fixed-shape spectra, only a qualitative statement of conservatism can be made about the 50^{th} and 84^{th} percentile spectra when used with a DSHA. However, a unique probability can be assigned to spectra computed by spectral attenuation expressions used in conjunction with a PSHA. A spectrum derived in this fashion is referred to as a uniform hazard spectrum (UHS) and is the topic of the next section.

6.4 Uniform hazard spectra

The response at each discrete frequency of a UHS has an equal probability of being exceeded. The steps involved in computing a UHS are the same as those for the probabilistic hazard curve described in Example 5.1, except the steps are repeated numerous times using different coefficients corresponding to each discrete frequency. Figure 6.1 shows the resulting site pseudo spectral velocity hazard curves for selected natural periods [National Research Council, 1988].

Unlike fixed-shaped spectra or spectra computed by spectral attenuation expressions used in conjunction with DSHA, a UHS may not be consistent in shape with response spectra derived from a

single earthquake time history. As a result, multiple real time histories or an artificial time history may be required if an in-depth dynamic analysis of the proposed structure were to be conducted, both of which have drawbacks. For complex structural systems (e.g., the piping in a nuclear power plant) the cost of performing multiple analyses using different time histories is both time consuming and expensive. Also, many engineers do not like using artificial time histories *because* they may not be representative of real earthquakes, especially where non-linear behavior is involved.

6.5 Description of Example 6.1

Examples 4.1 and 5.1 are continued in Example 6.1 with design spectra being derived using several approaches outlined below.

Scaled fixed-shape spectra:

- An 84th percentile Newmark-Hall spectrum (5 percent damping) scaled and anchored to the median PGA determined by DSHA procedures in Example 4.1.
- An 84th percentile Newmark-Hall spectrum (5 percent damping) scaled and anchored to the PGA associated with a 1000 year return period (or a probability of exceedance equal to 0.001) determined by PSHA procedures in Example 5.1.

Spectra obtained using spectral attenuation expressions in conjunction with a DSHA:

- An 84th percentile spectrum (5 percent damping) computed using Boore, Joyner & Fumal (1993) spectral attenuation expression applied in a DSHA fashion for the controlling earthquake determined in Example 4.1.
- An 84th percentile spectrum (5 percent damping) computed using Crouse (1991) spectral attenuation expression applied in a DSHA fashion for the controlling earthquake determined in Example 4.1.

Uniform hazard spectrum:

- A UHS associated with a 1000 year return period (or a

probability of exceedance equal to 0.001) is computed using Boore, Joyner, and Fumal (1993) spectral attenuation expression applied in a PSHA fashion.

When comparing the spectra at the end of Example 6.1, it must be kept in mind the source mechanisms corresponding to each. The spectrum computed using the Crouse (1991) spectral attenuation expression is for a subduction zone earthquake with a focal depth of 5 km. The spectra computed using the Boore, Joyner, and Fumal (1993) expression is for shallow crustal earthquakes, one of which is the UHS. Although the Newmark-Hall spectra is not specific for a given type of source mechanism, the PGA used in scaling and anchoring the spectra in this example were based on the Boore, Joyner, and Fumal (1993) acceleration attenuation expression.

Computation of the 84th percentile Newmark-Hall design response spectrum (5 percent damping) for the PGA determined in Example 4.1, (i.e., PGA = 0.22g) [Newmark, 1982].

STEP 1: Establish the PGA associated with design earthquake: The PGA associated with the design earthquake equals 0.22g.

STEP 2: Compute the peak ground velocity (PGV) and peak ground displacement (PGD):

$$v := c_1 \cdot \frac{a}{g} \qquad d := c_2 \cdot \frac{v^2}{a}$$

$c_1 := 36$ in/sec for rock sites, $c_2 := 6$ for both rock and soil sites,

a = PGA, v = PGV, d = PGD, and g = acceleration due to gravity. (NOTE: use consistent units.)

$a = 87$ in/sec^2 $\quad v = 8.1$ in/sec $\quad d = 4.5$ in

STEP 3: Compute the spectral values by multiplying the peak ground motion parameters by the respective amplification factors:

Compute the 84th percentile amplification factors:

$$\alpha_a := 4.38 - 1.04 \cdot \ln(\beta) \qquad \alpha_a = 2.706$$

$$\alpha_v := 3.38 - 0.67 \cdot \ln(\beta) \qquad \alpha_v = 2.302$$

$$\alpha_d := 2.73 - 0.45 \cdot \ln(\beta) \qquad \alpha_d = 2.006$$

β = percent of critical damping (i.e., 5%)

Compute the spectral values:

$$S_{pa} := \alpha_a \cdot \frac{a}{g} \qquad S_{pa} = 0.61\ g$$

$$S_{pv} := \alpha_v \cdot v \qquad S_{pv} = 19 \text{ in/sec}$$

$$S_d := \alpha_d \cdot d \qquad S_d = 9.0 \text{ in}$$

where S_{pa} = pseudo absolute acceleration,

S_{pv} = pseudo relative velocity, and

S_d = maximum relative displacement.

Example 6.1 Computation of site design spectra.

STEP 4: Determine f1, and 4*f1: f1 is the frequency corresponding to the intersection of lines with an amplitude of S_{pa} and S_{pv} , which are parallel to the acceleration and velocity axes, respectively, when plotted on tripartite log paper.

$f_1 = 2.2$ Hz (approximately)

Let: $f_2 = 4 \cdot f_1$ $f_2 = 8.8$ Hz

$f_3 = 33$ Hz

Repeat the steps for the PGA determined by Example 5.1 (PSHA: PGA = 0.34g)

$a = 130$ in/sec^2 $v = 12$ in/sec $d = 6.8$ in

$S_{pa} = 0.91$ g $S_{pv} = 28$ in/sec $S_d = 14$ in

$f_1 = 2.01$ Hz $f_2 = 8.04$ Hz $f_3 = 33$ Hz

The above information can be plotted as a series of straight lines directly on tripartite log paper with an x-axis in units of frequency, but in order to compare with the other spectra computed in this example the following approximate conversions will be made.

Period (sec)	pseudo relative velocity (cm/sec) for PGA=0.22g	Period (sec)	pseudo relative velocity (cm/sec) for PGA=0.34g
T_{NH1}	S_{pv1}	T_{NH2}	S_{pv2}
0.03	1.8	0.03	2.3
0.10	12.3	0.12	18.8
0.50	47.2	0.50	70.7
3.00	47.2	2.94	70.7
6.70	20.8	6.67	32.4

Example 6.1 (continued).

Computation of the 84th percentile design spectrum (5% damping) using the Boore, Joyner, and Fumal (1993) spectral attenuation expression in conjunction with the controlling earthquake determined in Example 4.1 (e.i., M = 7.5, R = 15 km) [Boore, 1993].

Boore, Joyner, and Fumal (1993):

$$\log(y) := b_1 + b_2 \cdot (M-6) + b_3 \cdot (M-6)^2 + b_4 \cdot \sqrt{R^2+h^2} + b_5 \cdot \log\left(\sqrt{R^2+h^2}\right) + b_6 \cdot G_B + b_7 \cdot G_C + \sigma_{logy}$$

$$S_{pv} := 10^{\log(y)}$$

where S_{pv} = pseudo relative velocity (cm/sec)

T=0.1sec

$b_1 := 1.7$ $b_2 := 0.321$ $b_3 := -0.104$ $b_4 := 0.0$ $b_5 := -0.921$ $b_6 := 0.039$
$b_7 := 0.128$ $h := 6.18$ $G_B := 0.0$ $G_C := 0.0$ $\sigma_{logy} := 0.194$

$$S_{pv_0} := 10^{logy} \qquad S_{pv_0} = 10.641$$

T=0.15sec

$b_1 := 1.956$ $b_2 := 0.323$ $b_3 := -0.117$ $b_4 := 0.0$ $b_5 := -0.939$ $b_6 := 0.137$
$b_7 := 0.217$ $h := 7.13$ $G_B := 0.0$ $G_C := 0.0$ $\sigma_{logy} := 0.194$

$$S_{pv_1} := 10^{logy} \qquad S_{pv_1} = 16.802$$

Example 6.1 (continued).

T=0.2sec

$b_1 := 2.042$ $b_2 := 0.332$ $b_3 := -0.112$ $b_4 := 0.0$ $b_5 := -0.931$ $b_6 := 0.185$

$b_7 := 0.274$ $h := 6.90$ $G_B := 0.0$ $G_C := 0.0$ $\sigma_{logy} := 0.196$

$S_{pv_2} := 10^{logy}$ $S_{pv_2} = 22.4$

T=0.3sec

$b_1 := 2.063$ $b_2 := 0.354$ $b_3 := -0.092$ $b_4 := 0.0$ $b_5 := -0.902$ $b_6 := 0.231$

$b_7 := 0.344$ $h := 5.79$ $G_B := 0.0$ $G_C := 0.0$ $\sigma_{logy} := 0.204$

$S_{pv_3} := 10^{logy}$ $S_{pv_3} = 31.839$

T=0.4sec

$b_1 := 2.029$ $b_2 := 0.373$ $b_3 := -0.072$ $b_4 := 0.0$ $b_5 := -0.876$ $b_6 := 0.252$

$b_7 := 0.388$ $h := 4.75$ $G_B := 0.0$ $G_C := 0.0$ $\sigma_{logy} := 0.211$

$S_{pv_4} := 10^{logy}$ $S_{pv_4} = 38.821$

T=0.7sec

$b_1 := 1.917$ $b_2 := 0.416$ $b_3 := -0.033$ $b_4 := 0.0$ $b_5 := -0.833$ $b_6 := 0.283$

$b_7 := 0.459$ $h := 3.08$ $G_B := 0.0$ $G_C := 0.0$ $\sigma_{logy} := 0.229$

$S_{pv_5} := 10^{logy}$ $S_{pv_5} = 51.121$

Example 6.1 (continued).

T=1sec

$b_1 := 1.858$ $b_2 := 0.444$ $b_3 := -0.016$ $b_4 := 0.0$ $b_5 := -0.825$ $b_6 := 0.305$

$b_7 := 0.497$ $h := 2.87$ $G_B := 0.0$ $G_C := 0.0$ $\sigma_{logy} := 0.245$

$$S_{pv_6} := 10^{logy} \qquad S_{pv_6} = 57.054$$

T=2sec

$b_1 := 1.905$ $b_2 := 0.491$ $b_3 := -0.028$ $b_4 := 0.0$ $b_5 := -0.898$ $b_6 := 0.381$

$b_7 := 0.554$ $h := 6.21$ $G_B := 0.0$ $G_C := 0.0$ $\sigma_{logy} := 0.287$

$$S_{pv_7} := 10^{logy} \qquad S_{pv_7} = 60.051$$

Computation of the 84th percentile design spectrum (5% damping) using the Crouse (1991) spectral attenuation expression in conjunction with the controlling earthquake determined in Example 4.1. A focal depth of h=5 km is used [Crouse, 1991].

Crouse (1991):

$$\ln(y) := b_1 - b_2 \cdot M + b_3 \cdot M^2 + b_4 \cdot \ln\left(R + b_5 \cdot \exp\left(b_6 \cdot M\right)\right) + b_7 \cdot h + \sigma_{lny}$$

$$S_{pv} := e^{\ln(y)}$$

where S_{pv} = pseudo relative velocity (cm/sec)

Example 6.1 (continued).

T = 0.1 sec

$b_1 := 3.26$ $b_2 := 1.12$ $b_3 := 0.0$ $b_4 := -1.93$ $b_5 := 1.58$ $b_6 := 0.608$

$b_7 := 0.00566$ $h := 5$ $M := 7.5$ $R := 15$ $\sigma_{lnPSV} = 0.738$

$S_{pv_0} := e^{lny}$ $S_{pv_0} = 12.929$

T = 0.2 sec

$b_1 := 4.44$ $b_2 := 1.09$ $b_3 := 0.0$ $b_4 := -1.92$ $b_5 := 1.58$ $b_6 := 0.608$

$b_7 := 0.00531$ $\sigma_{lnPSV} = 0.675$

$S_{pv_1} := e^{lny}$ $S_{pv_1} := 33.143$

T = 0.4 sec

$b_1 := 3.03$ $b_2 := 1.18$ $b_3 := 0.0$ $b_4 := -1.69$ $b_5 := 1.58$ $b_6 := 0.608$

$b_7 := 0.00357$ $\sigma_{lnPSV} = 0.637$

$S_{pv_2} := e^{lny}$ $S_{pv_2} := 49.183$

T = 0.6 sec

$b_1 := 2.86$ $b_2 := 1.41$ $b_3 := 0.0$ $b_4 := -1.93$ $b_5 := 1.58$ $b_6 := 0.608$

$b_7 := 0.00257$ $\sigma_{lnPSV} = 0.691$

$S_{pv_3} := e^{lny}$ $S_{pv_3} := 71.673$

Example 6.1 (continued).

T = 0.8 sec

$b_1 := 1.82$ $b_2 := 1.50$ $b_3 := 0.0$ $b_4 := -1.83$ $b_5 := 1.58$ $b_6 := 0.608$

$b_7 := 0.00215$ $\sigma_{lnPVS} = 0.705$

$S_{pv_4} := e^{lny}$ $S_{pv_4} = 84.154$

T = 1.0 sec

$b_1 := 1.43$ $b_2 := 1.56$ $b_3 := 0.0$ $b_4 := -1.83$ $b_5 := 1.58$ $b_6 := 0.608$

$b_7 := 0.00114$ $\sigma_{lnPSV} = 0.691$

$S_{pv_5} := e^{lny}$ $S_{pv_5} = 92.652$

T = 1.5 sec

$b_1 := -0.433$ $b_2 := 1.50$ $b_3 := 0.0$ $b_4 := -1.45$ $b_5 := 1.58$ $b_6 := 0.608$

$b_7 = 0.000843$ $\sigma_{lnPSV} = 0.736$

$S_{pv_6} := e^{lny}$ $S_{pv_6} = 62.578$

T =2.0 sec

$b_1 := -0.987$ $b_2 := 1.50$ $b_3 := 0.0$ $b_4 := -1.38$ $b_5 := 1.58$ $b_6 := 0.608$

$b_7 := -0.00220$ $\sigma_{lnPSV} = 0.719$

$S_{pv_7} := e^{lny}$ $S_{pv_7} = 50.214$

Example 6.1 (continued).

T =3.0 sec

$b_1 := -1.67 \quad b_2 := 1.59 \quad b_3 := 0.0 \quad b_4 := -1.41 \quad b_5 := 1.58 \quad b_6 := 0.608$

$b_7 := -0.00367 \qquad \sigma_{lnPSV} = 0.804$

$S_{pv_8} := e^{lny} \qquad S_{pv_8} := 46.197$

T =4.0 sec

$b_1 := -2.20 \quad b_2 := 1.67 \quad b_3 := 0.0 \quad b_4 := -1.46 \quad b_5 := 1.58 \quad b_6 := 0.608$

$b_7 := -0.00439 \qquad \sigma_{lnPSV} = 0.81$

$S_{pv_9} := e^{lny} \qquad S_{pv_9} := 38.447$

Uniform hazard spectrum (UHS): The Boore, Joyner, and Fumal (1993) spectral attenuation expression is used to compute the UHS. Each curve in the plot below is the P(Spv>v) for a descrete frequency. The steps involved in computing each of the curves are the same as those outlined in Example 5.1, except different coefficients are used. The point on each curve corresponding to a specified probability of exceedence (e.g., P(Spv>v) = 0.001) is just one point on the UHS. The UHS corresponding to a probability of exceedence of 0.001 is determined [Boore, 1993].

Boore, Joyner, and Fumal (1993):

$$\log(y) := b_1 - b_2 \cdot (M - 6) + b_3 \cdot (M - 6)^2 + b_4 \cdot \sqrt{R^2 + h^2}$$

$$+ \; b_5 \cdot \log\left(\sqrt{R^2 + h^2}\right) + b_6 \cdot G_B + b_7 \cdot G_C + \sigma_{logy}$$

The same values for the coefficients b_{1-7} and σ_{logy} used in computing the Boore, Joyner, and Fumal (1993) 84th percentile design spectrum deterministically above also are used in computing the site spectral pseudo relative velocity curves.

Example 6.1 (continued).

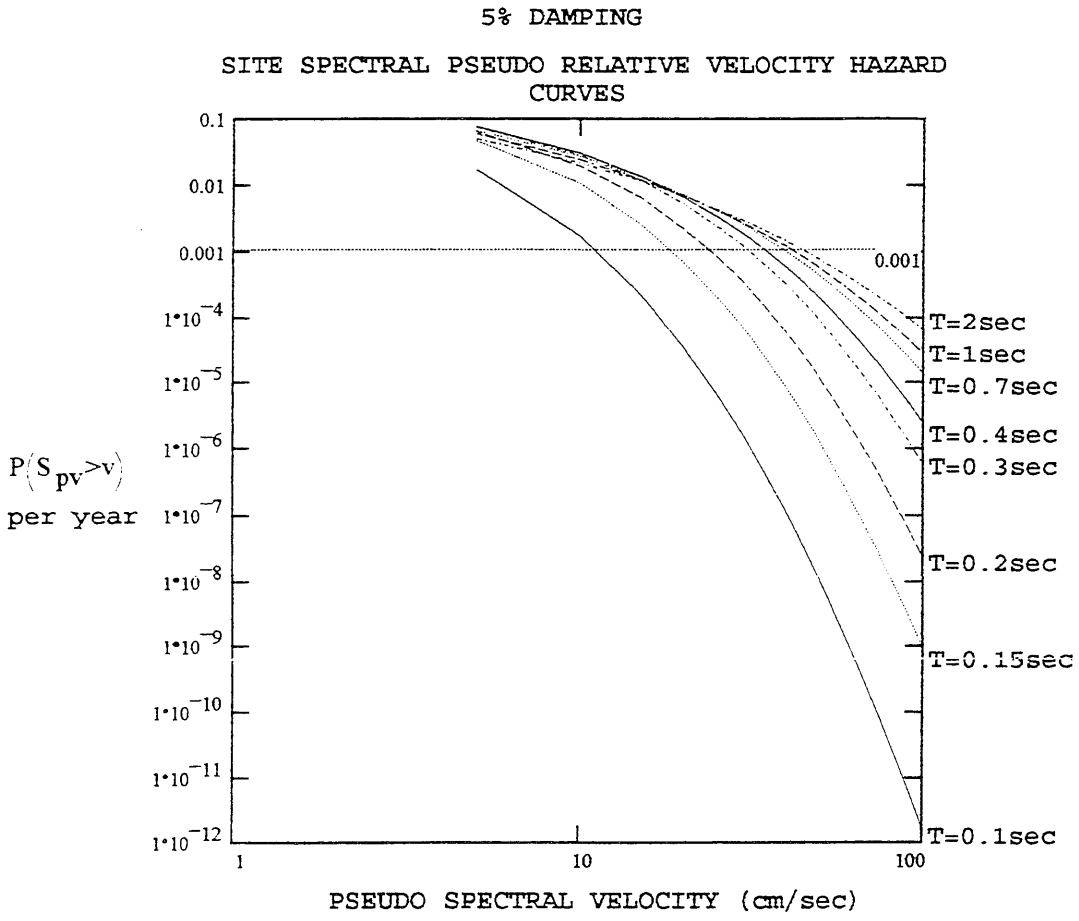

NOTE: The site hazard curves are derived using Boore, Joyner, and Fumal (1993) spectral attenuation expression.

Example 6.1 (continued).

Period (sec)	UHS S_{pv}: @ $P(S_{pv}>v)$ = 0.001 (cm/sec)
0.10	12.3
0.15	19.1
0.20	24.3
0.30	31.2
0.40	34.8
0.70	39.6
1.00	41.7
2.00	44.8

Summary of results:

Period (sec)	NH1 (cm/sec)	NH2 (cm/sec)	BJF (cm/sec)	Crouse (cm/sec)	UHS (cm/sec)
0.03	1.8	2.3	-	-	-
0.10	12	-	11	13	12
0.12	-	19	-	-	-
0.15	-	-	17	-	19
0.20	-	-	22	33	24
0.30	-	-	32	-	31
0.40	-	-	39	49	35
0.50	47	71	-	-	-
0.60	-	-	-	72	-
0.70	-	-	51	-	40
0.80	-	-	-	84	-
1.00	-	-	57	93	42
1.50	-	-	-	63	-
2.00	-	-	60	50	45
3.00	47	71	-	46	-
4.00	-	-	-	38	-
6.70	21	32	-	-	-

NH1 = 84th percentile Newmark-Hall spectrum scaled and anchored to PGA = 0.22g; DSHA. (approximate)

NH2 = 84th percentile Newmark-Hall spectrum scaled and anchored to PGA = 0.34g; PSHA. (approximate)

BJF = 84th percentile Boore, Joyner, and Fumal (1993) spectrum computed using R = 15km and M = 7.5;DSHA.

Crouse = 84th percentile Crouse (1991) spectrum computed using R =15km, M = 7.5, and h = 5km; DSHA.

UHS = Uniform Hazard Spectrum based on BJF for a $P(S_{pv}>v)$ = 0.001; PSHA

Example 6.1 (continued).

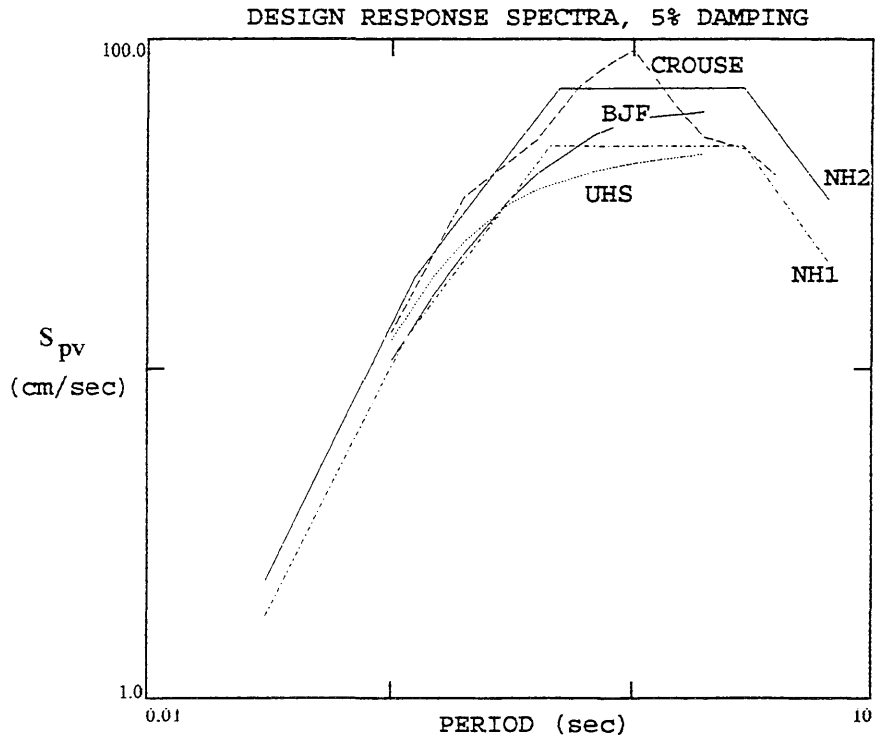

BJF = 84th percentile Boore, Joyner, and Fumal (1993)
Crouse = 84th percentile Crouse (1991)
NH1 = 84th percentile Newmark-Hall (PGA = 0.22g; DSHA)
NH2 = 84th percentile Newmark-Hall (PGA = 0.34g; PSHA)
UHS = Uniform Hazard Spectrum for 0.001 probability of exceedence, using BJF

NOTE: Both axes are log scales. For BJF and Crouse M=7.5 and R=15km. Also, for Crouse a subduction zone earthquake with a focal of h=5 km is used. The Uniform Hazard Spectrum is derived using Boore, Joyner, and Fumal (1993) spectral attenuation expression.

Example 6.1 (continued).

CHAPTER 7
CONCLUSION

7.1 Closing remarks

The purpose of this report was to provide the reader with an overview of the steps involved in selected methods of performing seismic hazard analyses. The issue as to which approach most accurately estimates the hazard at a given site is controversial, but no matter which approach is used, engineering judgement plays a key role. For example, in deterministic seismic hazard analyses, engineering judgement is needed in the selection of the design event's magnitude and distance, acceleration attenuation relationship, and type of design spectrum. The end result's sensitivity to each choice is generally easy to determine with minimal computational effort. As a result of this transparent cause-and-effect characteristic of DSHA, input decisions can be argued up-front with a clear understanding of their consequences.

In probabilistic seismic hazard analyses, engineering judgement is required in selecting the source boundaries, recurrence relationship, acceleration attenuation expression, forecasting model, and type of design spectrum. As opposed to DSHA, probabilistic analysis allows the integration of a wide range of possible choices, but the end result's sensitivity to each choice is generally difficult to discern. This obscurity of how varying an input affects the output (without performing a complete PSHA for various inputs), is probably the most unsettling characteristic of PSHA. Regardless of which method is employed, it should be kept in mind that the output of the analysis is only as good as its input.

LIST OF REFERENCES

[Abrahamson, 1994]
Norman Abrahamson, "Characterization of Earthquake Ground Motions," In *Proceedings: Advances in Earthquake Engineering Practice*, University of California, Berkeley, CA, May 31 to June 4, 1994.

[Ang, 1975]
Alfredo H-S. Ang and Wilson H. Tang, **Probability Concepts in Engineering Planning and Design, Volume I - Basic Principles**, John Wiley and Sons, New York, NY, 1975.

[Bolt, 1977]
B.A. Bolt, W.L. Horn, G.A. MacDonald, and R.F. Scott, **Geologic Hazards, Second Edition**, Springer-Verlag, New York Inc., New York, NY, 1977.

[Bolt, 1988]
Bruce A. Bolt, **Earthquakes**, W.H. Freeman and Company, New York, NY, 1988.

[Boore, 1983]
David M. Boore, "Stochastic Simulation of High-Frequency Ground Motions Based on Seismological Models of the Radiated Spectra," *BSSA*, Vol 73, No 6, 1983, pp. 1865-1894.

[Boore, 1986]
David M. Boore, "Short-period P- and S-wave radiation from large earthquakes: implications for spectral scaling relations," *BSSA*, Vol 76, No 1, 1986, pp. 43-64.

[Boore, 1993]
David M. Boore, William B. Joyner, and Thomas E. Fumal, Estimation of Response Spectra and Peak Accelerations From Western North American Earthquakes: An Interim Report, USGS Open-File Report 93-509, 1993.

[Clough, 1993]
Ray W. Clough and Joseph Penzien, **Dynamics of Structures, Second Edition**, McGraw-Hill, Inc., New York, NY, 1993.

[Cornell, 1968]
C. Allin Cornell, "Engineering Seismic Risk Analysis," *BSSA*, Vol 58, No 5, 1968, pp. 1583-1606.

[Cornell, 1988]
C.A. Cornell and S.R. Winterstein, "Temporal and magnitude dependence in earthquake recurrence models," *BSSA*, Vol 78, 1988, pp. 1522-1537.

[Cornell, 1993]
C. Allin Cornell, "Which 84th Percentile Do You Mean?," In Vol 1, *Proceedings: Fourth DOE Natural Phenomena Hazards Mitigation Conference*, CONF-9310102, October 19-22, 1993, pp. 152-159.

[Crouse, 1991]
C.B. Crouse, "Ground-Motion Attenuation Equations for Earthquakes on the Cascadia Subduction Zone," *Earthquake Spectra*, Vol 7, No 2, 1991, pp. 201-236.

[Donovan, 1978]
Neville C. Donovan and Ann E. Bornstein, "Uncertainties in Seismic Risk Procedures," *Journal of the Geotechnical Engineering Division, ASCE*, Vol 104, No GT7, 1978, pp. 869-887.

[Gere, 1984]
James M. Gere and Haresh C. Shah, **Terra Non Firma, Understanding and Preparing for Earthquakes**, W.H. Freeman and Company, New York, NY, 1984.

[Hall, 1976]
William J. Hall, Bijan Mohraz, and Nathan M. Newmark, Statistical Studies of Vertical and Horizontal Earthquake Spectra, NUREG-0003, U.S. Nuclear Regulatory Commission, 1976.

[Hanks, 1981]
Thomas C. Hanks and Robin K. McGuire, "The Character of High-Frequency Strong Ground Motion," *BSSA*, Vol 71, No 6, 1981, pp. 2071-2095.

[Hay, 1984]
Edward A. Hay and A. Lee McAlester, **Physical Geology, Principles and Perspectives, Second Edition**, Prentice-Hall, Inc., Englewood Cliffs, NJ, 1984.

[Housner, 1982]
G.W. Housner and P.C. Jennings, **Earthquake Design Criteria**, Earthquake Engineering Monograph Series, Earthquake Engineering Research Institute, 1982.

[Idriss, 1978]
I.M. Idriss, "Characteristics of Earthquake Ground Motions," In *Volume III, Proceeding of the ASCE Geotechnical Engineering Division Specialty Conference, EARTHQUAKE ENGINEERING AND SOIL DYNAMICS*, June 19-21, 1978, pp. 1151-1265.

[Krinitzsky, 1993a]
Ellis L. Krinitzsky, "Earthquake probability in engineering-Part 2: Earthquake recurrence and limitations of Gutenberg-Richter b-values for the engineering of critical structures," The Third Richard H. Jahns Distinguished Lecture in Engineering Geology, *Engineering Geology*, Vol 36, 1993, pp. 1-52.

[Krinitzsky, 1993b]
Ellis L. Krinitzsky, James P. Gould, and Peter H. Edinger, **Fundamentals of Earthquake Resistant Construction**, Wiley Series of Practical Construction Guides, John Wiley and Sons, Inc., New York, NY, 1993.

[Lindeburg, 1990]
Michael R. Lindeburg, **Seismic Design of Building Structures, Fifth Edition**, Professional Publications, Inc., Belmont, CA,

1990.

[McKenzie, 1980]
D.P. McKenzie and Frank Richter, "Convection Currents in the Earth's Mantle," Chapter 11, In **Earthquakes and Volcanoes**, Scientific American, Inc., W.H. Freeman and Company, San Francisco, 1980.

[National Research Council, 1988]
Probabilistic Seismic Hazard Analysis; Panel on Seismic Hazard Analysis; Committee on Seismology; Board on Earth Sciences; Commission on Physical Sciences, Mathematics, and Resources; Nation Research Council; National Academy Press, Washington, D.C., 1988.

[Newmark, 1973]
Nathan M. Newmark, John A. Blume, and Kanwar K. Kapur, "Seismic Design Spectra for Nuclear Power Plants," *Journal of the Power Division*, ASCE, Vol 99, No P02, 1973, pp. 287-303.

[Newmark, 1978]
Nathan M. Newmark and William J. Hall, Development of Criteria for Seismic Review of Selected Nuclear Power Plants, Nuclear Regulatory Commission Report NUREG/CR-0098, 1978.

[Newmark, 1982]
Nathan M. Newmark and William J. Hall, **Earthquakes Spectra and Design**, Earthquake Engineering Monograph Series, Earthquake Engineering Research Institute, 1982.

[Nuttli, 1978]
Otto W. Nuttli and Robert B. Herrmann, State-of-the-Art for Assessing Earthquake Hazards in the United States, Report 12, Credible Earthquakes for the Central United States, Miscellaneous Paper S-73-1, U.S. Army Engineer Waterways Experimental Station, Vicksburg, MS, 1978.

[Nuttli, 1987]
Otto W. Nuttli and Chiou-Fen Shieh, State-of-the-Art for Assessing Earthquake Hazards in the United States, Report 23, Empirical Study of Attenuation and Spectral Scaling Relations of Response Spectra for Western United States Earthquakes, Miscellaneous Paper S-73-1, U.S. Army Engineer Waterways Experimental Station, Vicksburg, MS, 1987.

[Richter, 1958]
Charles F. Richter, **Elementary Seismology**, W.H. Freeman and Company, San Francisco, CA, 1958.

[Reiter, 1990]
Leon Reiter, **Earthquake Hazard Analysis, Issues and Insights**, Columbia University Press, New York, NY, 1990.

[Silva, 1989]
Walter J. Silva, Robert B. Darragh, Robert K. Green, and F. Thomas Turcotte, Estimated Ground Motions for a New Madrid Event, Miscellaneous Paper GL-89-17, U.S. Army Engineer

Waterways Experimental Station, Vicksburg, MS, 1989.

[Silva, 1992]
Walter Silva, "Factors Controlling Strong Ground Motion and Their Associated Uncertainties," In *Proceedings: Dynamic Analysis and Design Considerations for HIGH-LEVEL NUCLEAR WASTE REPOSITORIES*, Structural Division/ASCE, San Francisco, CA, August 19-20, 1992, pp. 132-161.

[Tri-Service manual]
Technical Manual, Seismic Guidelines for Essential Buildings, Change 1, Army TM 5-809-10-1, Navy NAVFAC P-355.1, Air Force AFM 88-3, Chap. 13, Sec A, Departments of the Army, Navy, and Air Force, 1986.

[U.S. Atomic Energy Commission, 1973]
Nathan M. Newmark Consulting Engineering Services, A Study of Vertical and Horizontal Earthquake Spectra, WASH-1255, Directorate of Licensing, U.S. Atomic Energy Commission, Washington, D.C., 1973.

[Wells, 1994]
Donald L. Wells and Kevin J. Coppersmith, "New Empirical Relationships among Magnitude, Rupture Length, Rupture Width, Rupture Area, and Surface Displacement," *BSSA*, Vol 84, No 4, 1994, pp. 974-1002.